Journal of Medicinal Chemistry

Article

pubs.acs.org/jmc

Discovery of a Highly Tumor-Selective Organometallic Ruthenium(II)−Arene Complex

Catherine M. Clavel,[†] Emilia Păunescu,[†] Patrycja Nowak-Sliwinska,[†] Arjan W. Griffioen,[‡] Rosario Scopelliti,[†] and Paul J. Dyson*[,†]

[†]Institut des Sciences et Ingénierie Chimiques, Ecole Polytechnique Fédérale de Lausanne (EPFL), CH-1015 Lausanne, Switzerland

[‡]Angiogenesis Laboratory, Department of Medical Oncology, VUMC Cancer Center Amsterdam, 1081 HV Amsterdam, The Netherlands

Supporting Information

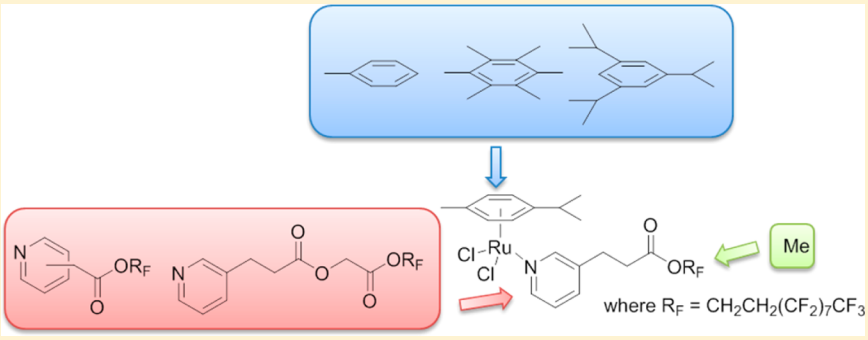

ABSTRACT: A ruthenium(II)−arene complex with a perfluoroalkyl-ligand was found to display remarkable selectivity toward cancer cells. IC_{50} values on several cancer cell lines are in the range of 25−45 μM, and no cytotoxic effect was observed on nontumorigenic (HEK-293) cells at concentrations up to 500 μM (the maximum concentration tested). Consequently, this complex was used as the basis for the development of a number of related derivatives, which were screened in cancerous and noncancerous cell lines. The lead compound was then evaluated in vivo for antiangiogenic activity in the CAM model and in a xenografted ovarian carcinoma tumor (A2780) grown on the CAM. A 90% reduction in the tumor growth was observed.

INTRODUCTION

Platinum-based drugs are widely used to treat cancer, but their therapeutic use can be impaired by intrinsic or acquired resistance and the occurrence of numerous side effects including nephrotoxicity, neurotoxicity, neuropathy, myelosuppresion, thrombocytopenia, and neutropenia.[1] The requirement for chemotherapeutic agents that are both active against platinum-resistant tumors and have superior therapeutic windows, i.e., leading to reduced side effects, gave rise to the emergence and rapid development of compounds based on other metals.[2] In particular, ruthenium complexes have attracted significant attention with two complexes, namely NAMI-A[3] and KP1019,[4] advancing through clinical trials. The latter compound is active against various primary tumors including those that respond poorly to existing chemotherapy regimens, whereas the first displays strong antimetastatic properties, both with relatively mild side effects.[5] The mechanism of action of these ruthenium(III) compounds, as well as others, has been widely studied in order to establish the basis for their unique properties, and it would appear that three main features are relevant: first, they interact with serum proteins such as albumin and transferrin that endows them with tumor seeking properties,[6] second, ruthenium(III) complexes appear to be activated through intracellular reduction to allow generation of toxic ruthenium(II) species,[7,8] and third, at the tumor site reactions (binding) with proteins are preferred to DNA binding, which contrasts with the behavior of platinum(II) complexes such as cisplatin.[9−11] Extrapolation of these pathways led to the direct evaluation of ruthenium(II) complexes and, in particular, organometallic ruthenium(II)−arene complexes.[12] On the basis of the general formula of half-sandwich ruthenium(II)−arene complexes, i.e., $[Ru(\eta^6\text{-arene})XYZ]^{n+}$ with X, Y, and Z being a combination of monodentate or bidentate/monodentate ligands, two main families of compounds have emerged with distinct modes of action. Compounds containing the bidentate ethylenediamine (en) ligand and a chloride, i.e., $[Ru(\eta^6\text{-arene})(en)Cl]^+$, are strongly cytotoxic in vitro,[13−15] whereas complexes with three monodentate ligands including a hydrophilic 1,3,5-triaza-7-phosphaadamantane (PTA) ligand, i.e., $[Ru(\eta^6\text{-arene})(PTA)Cl_2]$ (termed RAPTA), are not cytotoxic[16−18] but display relevant antimetastatic[16,19,20] and antiangiogenic[21] properties in vivo. Although the mechanism of action of this latter class of compounds remains unclear, it seems likely that RAPTA derivatives have a profoundly different biochemical mode of

Received: February 19, 2014
Published: March 26, 2014

dx.doi.org/10.1021/jm5002748 | J. Med. Chem. 2014, 57, 3546−3558

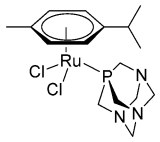

10 (RAPTA-C)

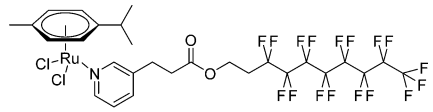

1

Figure 1. Structure of **10** (RAPTA-C) and **1**, the latter being used as a structural template for this study.

action to classical platinum anticancer agents.[22−24] In the nucleosome, for example, it has been shown that RAPTA compounds bind preferentially to the histone core relative to the DNA.[25] The identification of the full mechanism of action of RAPTA-like molecules is in progress,[23,26,27] as a better mechanistic understanding should help to improve the biological and pharmacological profile of these compounds.[28−32]

RAPTA complexes like RAPTA-C (**10**) are very hydrophilic and, recently, as part of our ongoing studies,[33] we turned our attention to bifunctional hydrophobic complexes, e.g. **1**, which carries a long fluorous chain (Figure 1). Indeed, **1** was selected as a promising lead drug candidate because it displays considerable selectivity toward tumor cells relative to model healthy cells. Moreover, in comparison to RAPTA compounds, **1** is substantially more cytotoxic to cisplatin-sensitive and cisplatin resistant ovarian cancer cells.[34] Herein, we describe the systematic modification of our lead drug candidate **1** and an in vitro and in vivo biological evaluation of this new compound class.

RESULTS AND DISCUSSION

Compound **1** comprises a ruthenium(II) center with an η^6-*p*-cymene ring, a fluorous-functionalized pyridine, and two chloride ligands. Each of these three ligand types was systematically modified: the *p*-cymene ligand in **1** was replaced by other arenes with varying steric bulk and the size, type, and position of the linker between the pyridine and the perfluorinated chain was also varied (see Scheme 1). The

Scheme 1. Chemical Modifications of 1

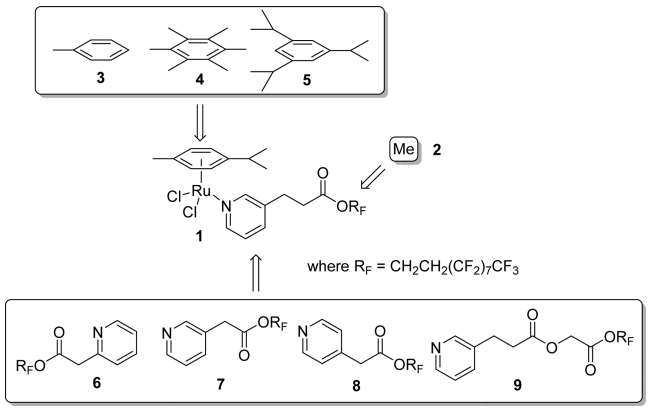

role of the perfluoro-alkyl chain with respect to the observed selectivity was also assessed by replacing it with a methyl group, i.e., in complex **2**. Complex **2** was obtained in good yield starting from commercially available methyl 3-(pyridin-3-yl)propanoate and the corresponding ruthenium dimer [(*p*-cymene)$RuCl_2$]$_2$.

Derivatives **3**−**5** were prepared to study the influence of the arene ring in comparison to *p*-cymene in **1** because the substituents on the arene influence cell uptake[14,16,35,36] and dissociation of the arene can take place upon binding of this type of complex to certain biomolecules,[37] and both these features influence the associated antiproliferative activity. Complexes **3**−**5** contain toluene, hexamethylbenzene, and 1,3,5-tri-*iso*-propylbenzene, respectively, and were synthesized in 66−97% yield from the pyridine ester ligand **5l**[33] and the appropriate arene dimers (Scheme 2).

Scheme 2. Synthesis of 3−5

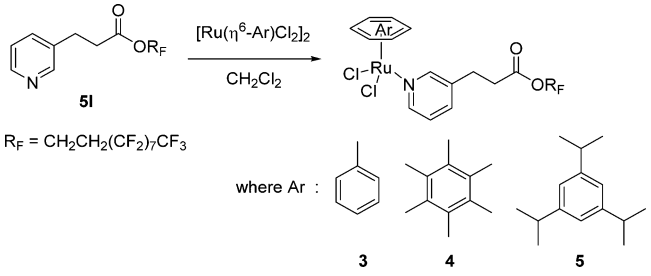

The pyridine ligand was also modified in a number of ways. A shorter carboxylate linker, acetate, was employed in **6**, **7**, and **8**, with the substitution position corresponding to ortho in **6**, meta in **7**, and para in **8**. The ortho (**1l**), meta (**2l**), and para (**3l**) substituted perfluorinated pyridine−acetate ligands were prepared from 1*H*,1*H*,2*H*,2*H*-perfluoro-1-decanol and the appropriate pyridine-acetic acid hydrochlorides in 66−86% yield. Ligand **4l**, with a supplementary glycolic ester group as a more hydrolytically cleavable linker between the pyridine moiety and the perfluorinated ponytail, was obtained following the three-step route shown in Scheme 3. Complexes **6**−**9** were obtained in good yield (72−97%) from the direct reaction of [(*p*-cymene)$RuCl_2$]$_2$ with the corresponding ligands, **1l**−**4l** (Scheme 3).

All the new compounds, **1l**−**4l** and **2**−**9**, were fully characterized by ^{1}H, ^{13}C and, where appropriate, ^{19}F NMR spectroscopy, ESI mass spectrometry, IR spectroscopy, and elemental analysis. As in the case of the previously described ligand **5l**, the formation of the perfluoroalkyl ester ligands **1l**−**4l** is accompanied by a deshielding of ca. 0.4 ppm of the methylene protons at the α position relative to the oxygen atom (as compared to 1*H*,1*H*,2*H*,2*H*-perfluoro-1-decanol). On formation of complexes **2**−**5**, **7**, and **9** (containing meta-substituted perfluoroalkylpyridine ligands), as well as in the case of complex **8** (which has a para-substituted perfluoroalkylpyridine ligand), a deshielding of ca. 0.4 ppm for the two protons at the α position to the nitrogen atom and of a deshielding of ca. 5 ppm for the respective carbon atoms is observed. Complex **6**, with an ortho-substituted perfluoroalkylpyridine ligand, exhibits some particularities, notably a smaller change in the frequencies of the ^{1}H and ^{13}C resonances

dx.doi.org/10.1021/jm5002748 | J. Med. Chem. 2014, 57, 3546−3558

Scheme 3. Synthesis of Ligands 1l–4l and Complexes 6–9

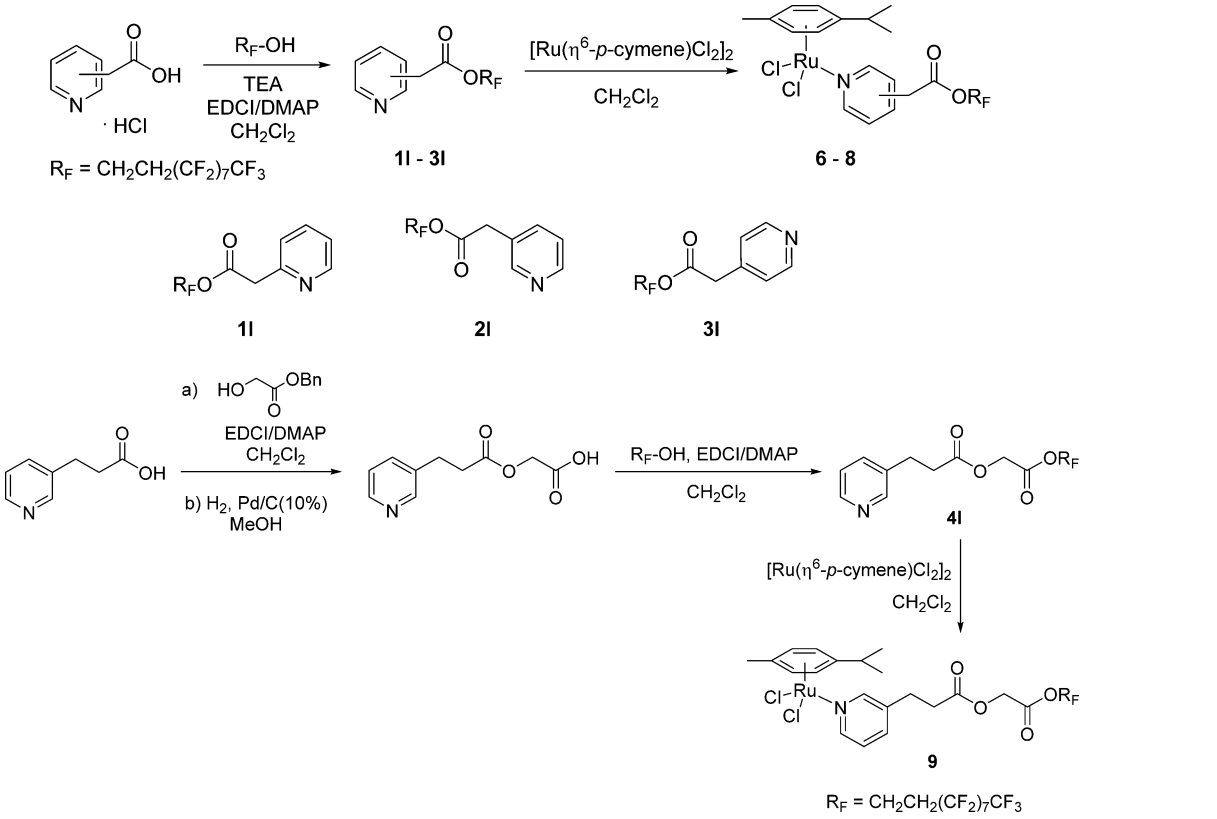

of the α position of the ligand with respect to the N atom. The resonances are also broad and poorly resolved, presumably due to the increased steric hindrance that impedes free rotation about the Ru–N bond and/or induces a rapid dissociation/reassociation process.

The ^{19}F NMR spectra of **1l–4l** and **3–9** and the very specific ^{13}C NMR spectroscopic profile confirm the presence of the fluorous chain. The fluorous chain is also evidenced from the IR spectra by the presence of a strong peak between 1110 and 1250 cm^{-1}. In the case of ligand **4l** and complex **9**, the second carboxylate group exhibits a shoulder at 1760–1770 cm^{-1} in the IR spectra, whereas the usual peak appears at 1744 cm^{-1}.

The structure of the compounds was also corroborated by ESI-MS. The most abundant peak observed in the spectra of the **1l–4l** are those assigned to $[M + H]^+$ ions, whereas the spectra of the complexes with two chlorine ligands were dominated by species assigned to $[M - Cl]^+$ ions.

Crystals suitable for X-ray diffraction were obtained for **2** by slow diffusion of hexane into a chloroform solution of the complex. The structure of **2** is shown in Figure 2, and key structural data are presented in Table 1.

Complex **2** adopts the familiar half-sandwich geometry with the bond parameters around the Ru center being remarkably similar to those of **10**[38,39] (see Table 1), indicating that the coordination sphere is largely preserved on replacing the P-donor ligand with the N-donor pyridine ligand.

In Vitro Antiproliferative Activity. The antiproliferative activity of the ligands **1l–5l** and their corresponding complexes, **1–9**, was evaluated in A2780 ovarian cancer cells and in the noncancerous human embryonic kidney (HEK-293) cell line (Table 2). Additional antiproliferative activity studies were performed on **1** in a broader panel of cancer cell lines including

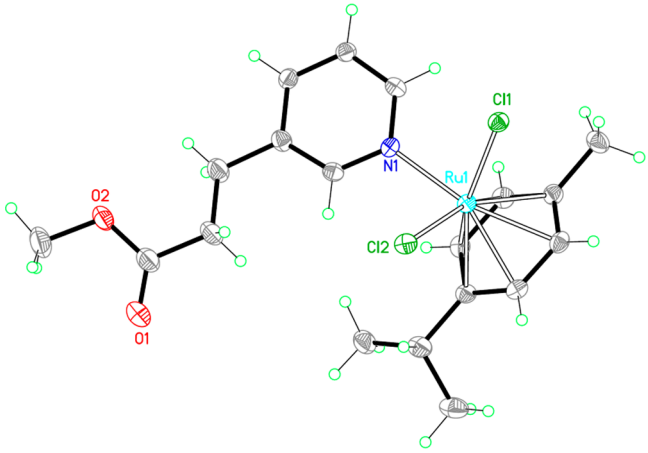

Figure 2. ORTEP representation of **2** (thermal ellipsoids are 30% equiprobability envelopes and H atoms are spheres of arbitrary diameter).

cisplatin-resistant ovarian carcinoma cells, breast cancer MCF-7 and MDA-MB-231 cell lines, and A549 lung cancer cells (Table 3).

The ligands are not particularly cytotoxic toward the A2780 cells, whereas the complexes display reasonable IC_{50} values ranging from 30.5 to 200 μM, all being considerably more cytotoxic than **10**.[31] Importantly, complexes **3** and **5–7** do not affect noncancerous cell proliferation, with IC_{50} values exceeding 500 μM (the highest concentration tested). The least active and least selective complex is **2**, which does not carry a perfluorinated chain. With respect to the other structural modifications, i.e., the influence of the arene, the substitution pattern on the pyridine ligand and the length of the alkyl chain

dx.doi.org/10.1021/jm5002748 | J. Med. Chem. 2014, 57, 3546–3558

Table 1. Key Bond Lengths (Å) and Angles (deg) of 2 and 10 for Comparison Purposes

	10[a]	2
Ru−η^6	1.692, 1.701	1.669(2)
Ru−P	2.296(2), 2.298(3)	
Ru−N		2.112(4)
Ru−Cl_{ave}	2.421, 2.426	2.4138(12)
Cl−Ru−Cl	87.25(8), 88.97(9)	87.64(4)
P−Ru−Cl_{ave}	84.01, 85.26	
N−Ru−Cl_{ave}		85.22(11)

[a]In the case of **10**, there are two independent molecules in the asymmetric unit. Taken from ref 38.

Table 2. IC_{50} Values for Ligands 1l−5l and Complexes 1−10 against the Ovarian Carcinoma A2780 and the Noncancerous HEK-293 Cell Lines after 72 h Determined Using the MTT Assay

compd	A2780 (μM)	HEK-293 (μM)
1l	157 ± 9	>500
2l	>500	>500
3l	>500	>500
4l	263 ± 24	60 ± 2
5l	263 ± 24	>500
1	44 ± 1	>500
2	200 ± 20	>500
3	87 ± 1	>500
4	65 ± 9	86 ± 3
5	31 ± 1	>500
6	177 ± 1	>500
7	97 ± 3	>500
8	71 ± 2	103 ± 12
9	40 ± 5	57 ± 5
10	251 ± 14	>500

Table 3. IC_{50} Values for 1 against Various Cancer Cell Lines Determined Using the MTT Assay after 72 h

	cell line			
	A2780cisR	MCF-7	MDA-MB-231	A549
1 (μM)	25 ± 2	38 ± 2	36 ± 2	43 ± 1

linker between the pyridine and ester moiety, there are not any clear trends that provide relevant structure−activity relationships, although these different structural features significantly alter anticancer activity while not changing the selectivity. In comparison to cisplatin, the IC_{50} in A2780 and HEK-293 cells correspond to 4.3 and 15.3 μM, respectively.[40]

The uptake of **1** and **3** into A2780 cells was determined following incubation for 24 h (Figure 3). A dose higher than the IC_{50} value of **1** and **3** was used as the incubation time was reduced. Compared to **10**, cell uptake of **1** and **3** is ca. 2-fold greater, which partially explains the superior cytotoxicity of the complexes. Cellular uptake of **1** was also quantified in the HEK-293 cells and is essentially the same as that determined in the A2780 cell line and, therefore, it is not possible to attribute the selective cytotoxicity of the compound to differences in uptake.

DNA profiles of propidium iodide (PI) stained A2780 cells treated with **1** were analyzed by flow cytometry in order to establish the mechanism of cell death (see Figure 4 and Table 4). Several reports indicate that ruthenium complexes inhibit the proliferation of cells by preventing cell cycle progression

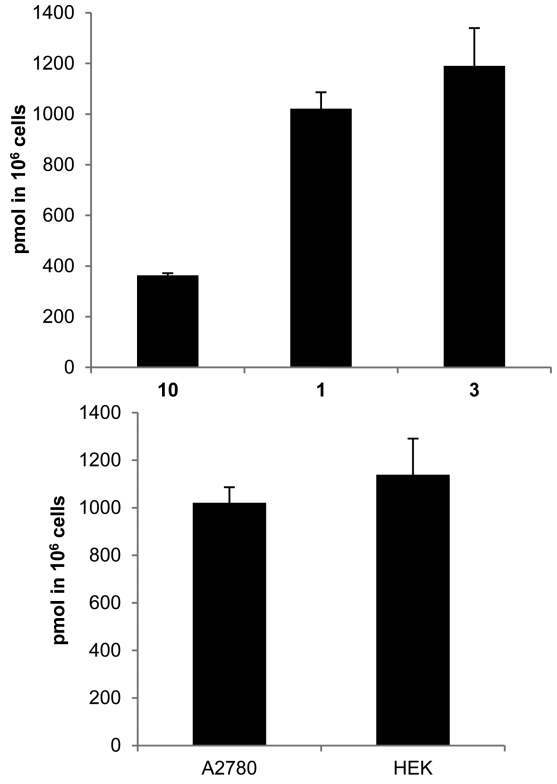

Figure 3. (top) Amount of **10**, **1**, and **3** (pmol in 10^6 cells) internalized in A2780 cells after 24 h (dose: 250 μM). (bottom) Uptake of **1** (pmol/10^6 cells) in A2780 and HEK-293 cells after a 24 h incubation (concentration: 250 μM).

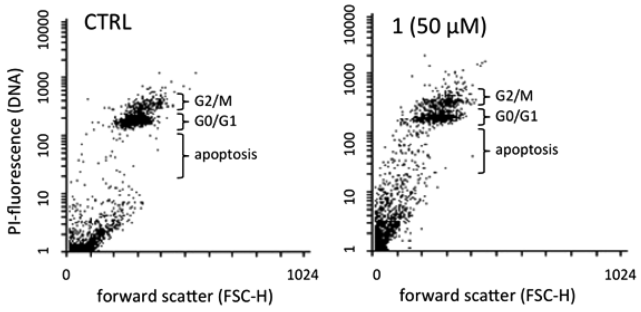

Figure 4. Comparison of DNA profiles from A2780 cells in the absence and presence of **1** (50 μM). Flow cytometry analysis of the DNA content after fixation of the A2780 cells in 70% ethanol, a DNA extraction step, and staining with PI. Control−solvent alone (left panel) and 50 μM of **1** (right panel) for 24 h.

Table 4. Cell-Cycle Changes in A2780 Cells by 1[a]

	1 (μM)		
	G1/G0 (±SD)	G2/M (±SD)	apoptosis (±SD)
DMSO 0.1%	69 ± 3	16.0 ± 1.4	2.0 ± 0.1
6	67.5 ± 0.7	21 ± 5	1.9 ± 0.3
12	69.0 ± 0.1	17.5 ± 0.7	2.2 ± 1.0
25	77.0 ± 1.4	17.0 ± 1.4	2.4 ± 0.4
50	59 ± 2	27.0 ± 0.1	6.4 ± 0.1

[a]The cell-cycle alterations were evaluated using PI-FACS analysis of A2780 cells (n = 4) after 24 h incubation of **1** at concentrations ranging from 6 to 50 μM.

dx.doi.org/10.1021/jm5002748 | J. Med. Chem. 2014, 57, 3546−3558

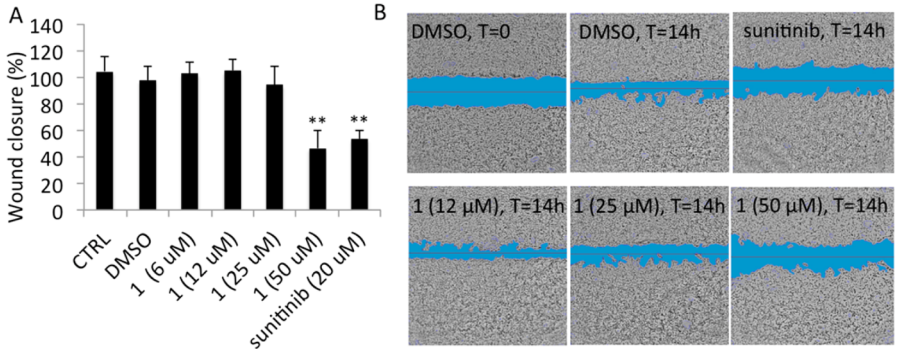

Figure 5. Assessment of migration inhibition of MDA-MB-231 cells after exposure to **1**. Wound closure in MDA-MB-231 cultures after 14 h of incubation with **1** at concentrations between 6 and 50 μM, DMEM culture medium, DMSO 0.1%, and sunitinib at 20 μM as a positive control. $^{**}P = 2.6 \times 10^{-7}$ (for **1**) and $^{**}P = 8.5 \times 10^{-8}$ (for sunitinib). Error bars represent standard error of the mean. (B) Typical images of the wound at the beginning of the experiment (0.1% DMSO solution in culture medium as a control) and after 14 h incubation with **1** or sunitinib.

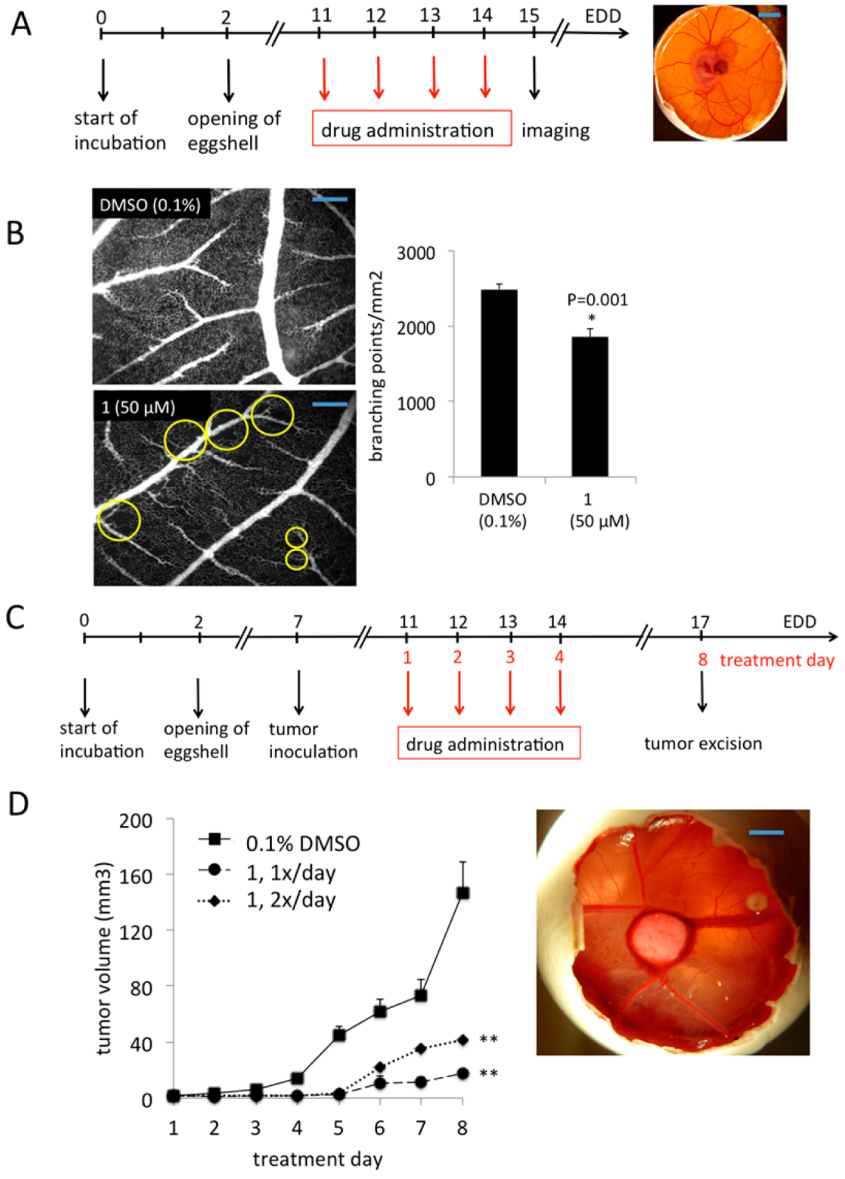

Figure 6. In vivo activity of **1** in the CAM model (A,B) and in xenografted ovarian tumors (A2780) grown on the CAM (C,D) using experimental protocol for the CAM only (A) or the tumor-bearing CAM (C), respectively. Complex **1** at 50 μM induced only mild, but statistically significant ($^{*}P = 1 \times 10^{-3}$) change in the vasculature architecture, compared to control (DMSO 0.1%), as quantified by measurement of the branching points (B). Tumor growth curves correspond to the following conditions: CTRL, **1** (50 μM; 100 μL, 1×/day, $^{**}P = 1.31 \times 10^{-5}$) or **1** (25 μM; 100 μL, 2×/day, $^{**}P = 7.12 \times 10^{-5}$). Error bars represent standard error of the mean. Bar stands for 5 mm (A,D) and 400 μm (B).

dx.doi.org/10.1021/jm5002748 | J. Med. Chem. 2014, 57, 3546−3558

and inducing apoptosis.[21,41,42] As reflected by the number of subdiploid cells (Figure 4 and Table 4), a moderate effect on apoptosis induction was observed at the 50 μM dose. Interestingly, incubation of A2780 cells with **1** (50 μM) for 24 h leads to an enhanced number of cells in the G2/M phase and a decrease of cells in the G1/G0 phase of cell cycle. Because **1** inhibits cell proliferation, this result most likely suggests that the compound synchronizes cells in the G2/M phase. Thus, **1** both induces apoptosis and prevents cell cycle progression. At lower doses, **1** did not induce apoptosis, neither did it cause significant changes of cells between cell cycle stages.

The effect of **1** on the motility of tumor cells was studied in a cell migration assay using invasive MDA-MB-231 human breast adenocarcinoma cells (Figure 5). At a concentration of 50 μM, **1** is able to significantly inhibit the migration capacity of tumor cells. The activity is comparable to that of sunitinib (at 20 μM), a clinically used antiangiogenic agent shown before to inhibit cell migration.[43] Representative images of the wounds before and after a 14 h incubation with a control solution (0.1% DMSO solution in culture medium), **1**, or sunitinib are shown in Figure 5B.

On the basis of its combined cellular effect, compound **1** was subsequently investigated in vivo using the chorioallantoic membrane (CAM) assay of the chicken embryo to evaluate the antiangiogenic potential (Figure 6). Initially, **1** was administered via a daily iv injection between EDD 11 and 14, followed by imaging of the CAM vasculature on EDD 15 (Figure 6A). A representative bright-field image of the fertilized embryo and the CAM at EDD 11 is shown in Figure 6A, and fluorescence angiographies of the CAM after the 4-day treatment, for 0.1% DMSO (CTRL) and **1** (50 μM), are shown in Figure 6B. A small but significant inhibitory effect on the vasculature was observed as avascular zones in the CAM (marked with yellow circles) for **1**, as compared to control treated CAMs. It should be noted that this effect is seen at the 50 μM dose, which is at least an order of magnitude lower than the concentration required to inhibit the growth of nontumorigenic HEK-293 cells. A reduction in the number of branching points per mm^2 of ca.10% was observed. To investigate the effect of **1** on tumor growth, A2780 ovarian carcinoma cells were inoculated at EDD 7 of the CAM and monitored for 11 days. Established and vascularized tumors were detected 3 days post implantation (EDD 10). Treatment was performed by iv injections on four consecutive days (Figure 6C). Tumors grew to an average size of approximately 150 mm^3 by EDD 17 when left untreated. Tumor growth was efficiently inhibited following treatment with **1**, performed 1×/day (50 μM), or 2×/day (2 × 25 μM, Figure 6D). On the last day of the experiment, the tumor growth was inhibited by approximately 90% ($^{**}P = 1.31 \times 10^{-5}$) at a dose of 1×/day (50 μM), whereas an inhibition of ca. 70% ($^{**}P = 7.12 \times 10^{-5}$) is observed at a dose of 2×/day (2 × 25 μM). The difference between an effect of **1** administrated once vs twice in a fractionated dose was also statistically significant ($^{**}P = 1.5 \times 10^{-4}$). The effect on the vasculature was only marginal (Figure 6B) as compared to the overall tumor growth inhibition (Figure 6D), confirming the antitumor activity of **1** in the absence of a strong antiangiogenic effect. Moreover, no detrimental side effects were observed during the treatment regimen. The dose applied for **1** is considerably lower than that employed with **10** in a engrafted mouse model (CBA mice bearing the MCa mammary carcinoma), which led to a reduction in the number and mass of metastatic tumors in the absence of an effect on the primary tumor.[44]

CONCLUSIONS

We disclose a ruthenium(II)−arene complex bearing a perfluorinated chain that displays remarkable selectivity toward cancer cells in vitro. At a noncytotoxic dose to healthy cells, the compound was evaluated for antiangiogenic and antitumoral activity in vivo. A modest antiangiogenic effect was observed, whereas a remarkable reduction in tumor growth, i.e., ca. 90%, was observed in the absence of measurable side effects. This behavior is quite distinct from that of **10**, in which the hydrophobic perfluoroalkyl-modified ligand in **1** is replaced by an amphiphilic 1,3,5-triaza-7-phosphaadamantane ligand in **10**. These differences in biological activity may therefore be, in part, due to increased uptake of **1** relative to **10**, although this does not fully explain the lack of toxicity observed in healthy cells. Nevertheless, further translational development of low molecular weight bifunctional ruthenium(II)−arene complexes is worthwhile as their low toxicity is attractive for development of future anticancer therapies. Moreover, it has been noted that the scarcity of in vivo studies on organometallic compounds in the literature is hindering the development of compounds with genuine clinical potential, as the majority of compounds that are active in vitro tend to be inactive in vivo,[45] limiting design strategies based entirely on in vitro data.

EXPERIMENTAL SECTION

General Procedures. $RuCl_3 \cdot 3H_2O$ was obtained from Precious Metals Online. Other chemical reagents were purchased from commercial sources (Aldrich, AlfaAesar, and Acros Chemicals) and used without further purification. Reactions were performed in solvents dried using a drying column and collected and used under an inert atmosphere of N_2. The dimers $[Ru(\eta^6\text{-toluene})Cl_2]_2$, $[Ru(\eta^6\text{-}p\text{-cymene})Cl_2]_2$, $[Ru(\eta^6\text{-hexamethylbenzene})Cl_2]_2$, and $[Ru(\eta^6\text{-1,3,5-tri-}iso\text{-propyl-benzene})Cl_2]_2$ were prepared and purified according to literature procedures.[46−50] The synthesis of **1** and of the corresponding ligand has been reported previously.[33] Reactions were performed under N_2 using Schlenk technique, and the complexation reactions and manipulation of the ruthenium dimers and complexes were performed in the absence of light. The synthesis of the ligands was monitored by TLC using Merck TLC Silicagel coated aluminum sheets 60 F_{254}, using UV lamp at 254 nm and $KMnO_4$ stain for visualization, and using hexane/EtOAc mixture as eluent. Purification of the ligands was carried out by flash column chromatography using a Varian 971-FP Autocolumn purification machine and prepacked Silicagel columns (Luknova flash columns (40−60 μm)) using a hexane/EtOAc mixture in gradient as the eluent. ^{1}H (400.13 MHz), ^{19}F (375.46 MHz), and ^{13}C (100.62 MHz) NMR spectra were recorded on a Bruker Avance II 400 spectrometer at 298 K. The chemical shifts are reported in parts per million (ppm) and referenced to deuterated solvent residual peaks ($CDCl_3$: ^{1}H δ 7.26, ^{13}C δ 77.16 ppm),[51] and coupling constants (J) are reported in hertz (Hz). IR spectra were recorded on a PerkinElmer Spectrum One FT-IR spectrometer at room temperature. High resolution electrospray ionization mass spectra (HR ESI-MS) were obtained on a Thermo-Finnigan LCQ Deca XP Plus quadropole ion-trap instrument operated in positive-ion mode. Elemental analyses were carried out at the microanalytical laboratory at the Institute of Chemical Sciences and Engineering (EPFL). Melting points were determined using a SMP3 Stuart melting point apparatus and are uncorrected. Compound purity was confirmed by elemental analysis with a minimum percentage of 95%.

Synthesis of $[Ru(\eta^6\text{-}p\text{-cymene})Cl_2$(methyl-3-(pyridin-3-yl)-propanoate)] 2. To a solution of $[Ru(\eta^6\text{-}p\text{-cymene})Cl_2]_2$ (1 equiv, 0.530 g, 0.865 mmol) in CH_2Cl_2 (10 mL), a solution of methyl-3-(pyridin-3-yl)propanoate (2.1 equiv, 0.300 g, 1.816 mmol) in CH_2Cl_2 (20 mL) was added, and the resulting mixture stirred at rt in the dark for about 4 days. The reaction mixture was concentrated under reduced pressure almost to dryness. Several drops of Et_2O were added

dx.doi.org/10.1021/jm5002748 | J. Med. Chem. 2014, 57, 3546−3558

to afford an orange precipitate that was washed with Et_2O (3 × 20 mL), hexane (20 mL), and again Et_2O (20 mL). The orange solid was removed by filtration and dried under a flow of N_2. The procedure was repeated twice to afford the product as an orange solid (0.660 g, η = 77%); mp (°C) 132.5−134.

^{1}H NMR ($CDCl_3$) δ_H, ppm: 8.90 (1H, s, N_{py}-C*H*-C), 8.87 (1H, d, N_{py}-C*H*-CH, $^3J_{H,H}$ = 5.4 Hz), 7.57 (1H, d, N_{py}-CH-C-C*H*, $^3J_{H,H}$ = 7.8 Hz), 7.22 (1H, dd overlapped, N_{py}-CH-C*H*, $^3J_{H,H}$ = 7.8 Hz, $^3J_{H,H}$ = 5.6 Hz), 5.42 (2H, d, 2 × CH_3-C-CH-C*H*(*Ar*), $^3J_{H,H}$ = 5.8 Hz), 5.21 (2H, d, 2 × CH_3-C-C*H*(*Ar*), $^3J_{H,H}$ = 5.8 Hz), 3.66 (3H, s, O-CH_3), 2.92−2.99 (1H, m, *Ar*-C*H*(CH_3)$_2$), 2.94 (2H, t, *Py*-CH_2-CH_2-C═O, $^3J_{H,H}$ = 7.2 Hz), 2.64 (2H, t, *Py*-CH_2-CH_2-C═O, $^3J_{H,H}$ = 7.2 Hz), 2.07 (3H, s, *Ar*-CH_3), 1.29 (6H, d, *Ar*-CH(CH_3)$_2$, $^3J_{H,H}$ = 7.1 Hz).

^{13}C NMR ($CDCl_3$) δ_C, ppm: 172.4 (1C, CH_2-C═O), 154.9 (1C, N_{py}-CH-C), 152.8 (1C, N_{py}-CH-CH), 137.7 (1C, N_{py}-CH-C-CH), 137.1 (1C, N_{py}-CH-C-CH), 124.2 (1C, N_{py}-CH-CH), 103.3 (1C, CH_3-C-CH-CH-C(*Ar*)), 97.2 (1C, CH_3-C-CH(*Ar*)), 82.9 (2C, 2 × CH_3-C-CH-CH(*Ar*)), 82.2 (2C, 2 × CH_3-C-CH(*Ar*)), 51.8 (1C, O-CH_3), 34.5 (1C, *Py*-CH_2-CH_2-C═O), 30.6 (1C, *Ar*-CH(CH_3)$_2$), 27.7 (1C, *Py*-CH_2-CH_2-C═O), 22.3 (2C, *Ar*-CH(CH_3)$_2$), 18.1 (1C, *Ar*-CH_3).

IR (ν, cm^{-1}): 3274 (CH-*Ar*), 3059, 2874 (CH_2,CH, CH_3), 1727 (C═O), 1473, 1421 (*Py* C═C, C═N), 1267 (C−O). ESI-MS(+): *m*/*z* found 436.07 [M-Cl]$^+$, calcd for $C_{19}H_{25}ClNO_2$ Ru 436.06, the experimental isotopic pattern fits well the calculated one. Anal. (%) Calcd for $C_{19}H_{25}Cl_2NO_2$Ru: C 48.41, H 5.35, N 2.97. Found: C 48.46, H 5.15, N 3.04.

General Procedure for the Synthesis of [Ru(η^6-arene)-Cl_2(1*H*,1*H*,2*H*,2*H*-perfluorodecyl-3-(pyridin-3-yl)propanoate)] (Where Arene = Toluene, Hexamethylbenzene, 1,3,5-Tri-*iso*-propylbenzene) 3−5. To a solution (or suspension) of the appropriate ruthenium(II)−arene dimer [Ru(η^6-arene)Cl_2]$_2$ (1 equiv) in CH_2Cl_2 (10 mL), a solution of 1*H*,1*H*,2*H*,2*H*-perfluorodecyl-3-(pyridin-3-yl)propanoate (**5l**) (2.1 equiv) in CH_2Cl_2 (20 mL) was added and the reaction mixture was stirred at rt in the dark for about 4 days. The reaction mixture was then concentrated under reduced pressure almost to dryness and the product precipitated with Et_2O. The resulting precipitate was washed with Et_2O (3 × 20 mL), hexane (20 mL), and again Et_2O (20 mL), then removed by filtration and dried under a flow of N_2.

[Ru(η^6-toluene)Cl_2(1H,1H,2H,2H-perfluorodecyl-3-(pyridin-3-yl)-propanoate)] ***3***. [Ru(η^6-toluene)Cl_2]$_2$ (0.190 g, 0.359 mmol) and 1*H*,1*H*,2*H*,2*H*-perfluorodecyl-3-(pyridin-3-yl)propanoate (**5l**) (0.450 g, 0.753 mmol) were used. The product was obtained as orange solid (0.566 g, η = 92%); mp (°C) 150−151.5.

^{1}H NMR ($CDCl_3$) δ_H, ppm: 8.95 (1H, s, N_{py}-C*H*-C), 8.92 (1H, d, N_{py}-C*H*-CH, $^3J_{H,H}$ = 5.6 Hz), 7.59 (1H, d, N_{py}-CH-C-C*H*, $^3J_{H,H}$ = 7.8 Hz), 7.24 (1H, dd, N_{py}-CH-C*H*, $^3J_{H,H}$ = 7.8 Hz, $^3J_{H,H}$ = 5.6 Hz), 5.64 (2H, dd overlapped, 2 × CH_3-C-CH-C*H* (*Ar*), $^3J_{H,H}$ = 5.5 Hz), 5.53 (1H, dd overlapped, CH_3-C-CH-CH-C*H* (*Ar*), $^3J_{H,H}$ = 5.5 Hz), 5.27 (2H, d, 2 × CH_3-C-C*H* (*Ar*), $^3J_{H,H}$ = 5.5 Hz), 4.38 (2H, t, O-CH_2-CH_2, $^3J_{H,H}$ = 6.5 Hz), 2.96 (2H, t, *Py*-CH_2-CH_2-C═O, $^3J_{H,H}$ = 7.2 Hz), 2.67 (2H, t, *Py*-CH_2-CH_2-C═O, $^3J_{H,H}$ = 7.2 Hz), 2.41−2.53 (2H, m, O-CH_2-CH_2), 2.13 (3H, m, *Ar*-CH_3).

^{13}C NMR ($CDCl_3$) δ_C, ppm: 171.6 (1C, CH_2-C═O), 155.1 (1C, N_{py}-CH-C), 153.2 (1C, N_{py}-CH-CH), 137.8 (1C, N_{py}-CH-C-CH), 137.0 (1C, N_{py}-CH-C-CH), 124.3 (1C, N_{py}-CH-CH), 104.8−121.7 (8C, m series, CH_2-CF_2-CF_2, CH_2-CF_2-CF_2, CH_2-$(CF_2)_2$-CF_2, CH_2-$(CF_2)_3$-CF_2, CF_2-$(CF_2)_2$-CF_3, CF_2-CF_2-CF_3, CF_2-CF_2-CF_3, CF_2-CF_2-CF_3), 100.3 (1C, CH_3-C-CH(*Ar*)), 87.3 (2C, 2 × CH_3-C-CH-CH(*Ar*)), 81.2 (2C, 2 × CH_3-C-CH-CH(*Ar*)), 79.7 (1C, CH_3-C-CH-CH-CH(*Ar*)), 56.6 (1C, t, O-CH_2-CH_2, $^3J_{C,F}$ = 4 Hz), 34.6 (1C, *Py*-CH_2-CH_2-C═O), 30.5 (1C, t, O-CH_2-CH_2, $^2J_{C,F}$ = 22 Hz), 27.6 (1C, *Py*-CH_2-CH_2-C═O), 18.8 (1C, *Ar*-CH_3).

^{19}F NMR ($CDCl_3$) δ_F, ppm: −80.76 (3F, t, CF_3, $^3J_{F,F}$ = 9.9 Hz), −113.62 (2F, m, CH_2-CF_2-CF_2), −121.64 (2F, m, CH_2-$(CF_2)_2$-CF_2), −121.90 (4F, m, CH_2-$(CF_2)_3$-CF_2, CH_2-$(CF_2)_4$-CF_2), −122.71 (2F, m, CF_2-CF_2-CF_3), −123.52 (2F, m, CH_2-CF_2-CF_2), −126.10 (2F, m, CF_2-CF_3).

IR (ν, cm^{-1}): 3059 (CH-*Ar*), 2956−2852 (CH_2, CH_3), 1739 (C═O), 1477, 1440, 1418 (C═C, C═N), 1367, 1329, 1115−1244 (CF_2, CF_3), 1197 (C−O). ESI-MS(+): *m*/*z* found 825.93 [M − Cl]$^+$, calcd for $C_{25}H_{20}ClF_{17}NO_2Ru$ 825.99, the experimental isotopic pattern fits well the calculated one. Anal. (%) Calcd for $C_{25}H_{20}Cl_2F_{17}NO_2Ru$ C 34.86, H 2.34, N 1.63; found C 37.75, H 2.77, N 1.64.

[Ru(η^6-hexamethylbenzene)Cl_2(1H,1H,2H,2H-perfluorodecyl-3-(pyridin-3-yl)propanoate)] ***4***. [Ru(η^6-hexamethylbenzene)Cl_2]$_2$ (0.09 g, 0.135 mmol) and 1*H*,1*H*,2*H*,2*H*-perfluorodecyl-3-(pyridin-3-yl)-propanoate (**5l**) (0.169 g, 0.283 mmol) were used. The product was isolated as an orange solid (0.166 g, η = 66%); mp (°C) 162−163.5.

^{1}H NMR ($CDCl_3$) δ_H, ppm: 8.64−8.66 (1H, m, N_{py}-C*H*-C, N_{py}-C*H*-CH), 7.54 (1H, d, N_{py}-CH-C-C*H*, $^3J_{H,H}$ = 7.2 Hz), 7.20 (1H, dd overlapped, N_{py}-CH-C*H*, $^3J_{H,H}$ = 7.2 Hz), 4.37 (2H, t, O-CH_2-CH_2, $^3J_{H,H}$ = 6.4 Hz), 2.93 (2H, t, *Py*-CH_2-CH_2-C═O, $^3J_{H,H}$ = 7.2 Hz), 2.65 (2H, t, *Py*-CH_2-CH_2-C═O, $^3J_{H,H}$ = 7.2 Hz), 2.42−2.51 (2H, m, O-CH_2-CH_2), 1.97 (18H, s, 6 × *Ar*-CH_3).

^{13}C NMR ($CDCl_3$) δ_C, ppm: 171.7 (1C, CH_2-C═O), 154.6 (1C, N_{py}-CH-C), 152.8 (1C, N_{py}-CH-CH), 137.4 (1C, N_{py}-CH-C-CH), 136.9 (1C, N_{py}-CH-C-CH), 124.2 (1C, N_{py}-CH-CH), 104.8−121.9 (8C, m series, CH_2-CF_2-CF_2, CH_2-CF_2-CF_2, CH_2-$(CF_2)_2$-CF_2, CH_2-$(CF_2)_3$-CF_2, CF_2-$(CF_2)_2$-CF_3, CF_2-CF_2-CF_3, CF_2-CF_2-CF_3, CF_2-CF_2-CF_3), 91.3 (6C, 6 × C-CH_3(*Ar*)), 56.7 (1C, t, C-i, $^3J_{C,F}$ = 4 Hz, O-CH_2-CH_2), 34.6 (1C, *Py*-CH_2-CH_2-C═O), 30.5 (1C, t, O-CH_2-CH_2, $^2J_{C,F}$ = 22 Hz), 27.6 (1C, *Py*-CH_2-CH_2-C═O), 15.4 (6C, 6 × CH_3-C(*Ar*)).

^{19}F NMR ($CDCl_3$) δ_F, ppm: −80.72 (3F, t, CF_3, $^3J_{F,F}$ = 9.7 Hz), −113.58 (2F, m, CH_2-CF_2-CF_2), 121.62 (2F, m, CH_2-$(CF_2)_2$-CF_2), −121.87 (4F, m, CH_2-$(CF_2)_3$-CF_2, CH_2-$(CF_2)_4$-CF_2), −122.67 (2F, m, CF_2-CF_2-CF_3), −123.49 (2F, m, CH_2-CF_2-CF_2), −126.07 (2F, m, CF_2-CF_3).

IR (ν, cm^{-1}): 3065−2923 (CH-*Ar*, CH_2, CH_3), 1741 (C═O), 1430−1474 (C═C, C═N), 1371, 1115−1242 (CF_2, CF_3), 1199 (C−O). ESI-MS(+): *m*/*z* found 896.07 [M − Cl]$^+$, calcd for $C_{30}H_{30}ClF_{17}NO_2Ru$ 896.07, the experimental isotopic pattern fits well the calculated one. Anal. (%) Calcd for $C_{30}H_{30}Cl_2F_{17}NO_2Ru$: C 38.68, H 3.25, N 1.50. Found: C 39.94, H 2.95, N 1.53.

[Ru(η^6-1,3,5-tri-iso-propylbenzene)Cl_2(1H,1H,2H,2H-perfluorodecyl-3-(pyridin-3-l)propanoate)] ***5***. [Ru(η^6-1,3,5-tri-*iso*-proylbenzene)-Cl_2]$_2$ (0.270 g, 0.359 mmol) and 1*H*,1*H*,2*H*,2*H*-perfluorodecyl-3-(pyridin-3-yl)propanoate (**5l**) (0.450 g, 0.753 mmol) were used. The product was isolated as an orange solid (0.689 g, η = 97%); mp (°C) 112.5−113.5.

^{1}H NMR ($CDCl_3$) δ_H, ppm: 8.95 (1H, s, N_{py}-C*H*-C), 8.91 (1H, d, N_{py}-C*H*-CH, $^3J_{H,H}$ = 7.5 Hz), 7.55 (1H, d, N_{py}-CH-C-C*H*, $^3J_{H,H}$ = 6.7 Hz), 7.19 (1H, dd overlapped, N_{py}-CH-C*H*, $^3J_{H,H}$ = 7.5 Hz), 4.38 (2H, t, O-CH_2-CH_2, $^3J_{H,H}$ = 6.5 Hz), 2.94 (2H, t, *Py*-CH_2-CH_2-C═O, $^3J_{H,H}$ = 7.2 Hz), 2.79−2.87 (3H, sept, 3 × *Ar*-C*H*(CH_3)$_2$, $^3J_{H,H}$ = 6.8 Hz), 2.65 (2H, t, *Py*-CH_2-CH_2-C═O, $^3J_{H,H}$ = 7.2 Hz), 2.41−2.53 (2H, m, O-CH_2-CH_2), 1.25 (18H, d, 3 × *Ar*-CH(CH_3)$_2$, $^3J_{H,H}$ = 6.8 Hz).

^{13}C NMR ($CDCl_3$) δ_C, ppm: 171.7 (1C, CH_2-C═O), 155.3 (1C, N_{py}-CH-C), 153.4 (1C, N_{py}-CH-CH), 137.6 (1C, N_{py}-CH-C-CH), 136.7 (1C, N_{py}-CH-C-CH), 124.0 (1C, N_{py}-CH-CH), 106.8−120.5 (8C, m series, CH_2-CF_2-CF_2, CH_2-CF_2-CF_2, CH_2-$(CF_2)_2$-CF_2, CH_2-$(CF_2)_3$-CF_2, CF_2-$(CF_2)_2$-CF_3, CF_2-CF_2-CF_3, CF_2-CF_2-CF_3, CF_2-CF_2-CF_3), 107.5 (3C, 3 × *Ar*-C-CH(CH_3)$_2$), 75.3 (3C, 3 × CH-C(*Ar*)), 56.8 (1C, t, O-CH_2-CH_2, $^3J_{C,F}$ = 4 Hz), 34.6 (1C, *Py*-CH_2-CH_2-C═O), 31.0 (3C, 3 × *Ar*-CH(CH_3)$_2$), 30.6 (1C, t, O-CH_2-CH_2, $^2J_{C,F}$ = 23 Hz), 27.7 (1C, *Py*-CH_2-CH_2-C═O), 22.4 (6C, 3 × *Ar*-CH(CH_3)$_2$).

^{19}F NMR ($CDCl_3$) δ_F, ppm: −80.73 (3F, t, CF_3, $^3J_{F,F}$ = 9.7 Hz), −113.62 (2F, m, CH_2-CF_2-CF_2), −121.62 (2F, m, CH_2-$(CF_2)_2$-CF_2), −121.88 (4F, m, CH_2-$(CF_2)_3$-CF_2, CH_2-$(CF_2)_4$-CF_2), −122.67 (2F, m, CF_2-CF_2-CF_3), −123.49 (2F, m, CH_2-CF_2-CF_2), −126.07 (2F, m, CF_2-CF_3).

IR (ν, cm^{-1}): 2874−3032 (CH-*Ar*, CH_2, CH, CH_3), 1747 (C═O), 1516, 1467−1416 (*Py* C═C, C═N), 1360, 1244−1115 (CF_2, CF_3), 1195 (C−O). ESI-MS(+): *m*/*z* found 938.12 [M − Cl]$^+$, calcd for $C_{33}H_{36}ClF_{17}NO_2Ru$ 938.12, the experimental isotopic pattern fits well the calculated one. Anal. (%) Calcd for $C_{33}H_{36}Cl_2F_{17}NO_2Ru$: C 40.71, H 3.73, N 1.44. Found: C 40.58, H 3.51, N 1.49.

dx.doi.org/10.1021/jm5002748 | *J. Med. Chem.* 2014, 57, 3546−3558

General Procedure for the Synthesis of the Ester Ligands 1l−3l. TEA (1 equiv) was added to a suspension of the appropriate 2-(pyridinyl)acetic acid hydrochloride (1 equiv) in dry CH_2Cl_2 (50 mL) at 0 °C, and the mixture was stirred at rt for 20 min. EDCI (1 equiv), 1*H*,1*H*,2*H*,2*H*-perfluoro-1-decanol (1 equiv), and 4-(dimethylamino)-pyridine (DMAP) (0.2 equiv) were sequentially added, and the resulting mixture was stirred at rt for ca. 4 days. The mixture was then diluted with CH_2Cl_2 (100 mL) and washed with H_2O (100 mL), and the aqueous phase was re-extracted with CH_2Cl_2 (2 × 100 mL) and the combined organic phases washed with brine (150 mL), dried over anhydrous Na_2SO_4, and concentrated under reduced pressure. Solid deposition on Celite and purification by flash chromatography afforded the desired compounds.

1H,1H,2H,2H-Perfluorodecyl-2-(pyridin-2-yl)acetate ***1l.*** 2-(Pyridine-2-yl)acetic acid hydrochloride (0.500 g, 2.880 mmol), TEA (0.400 mL, 2.880 mmol), 1*H*,1*H*,2*H*,2*H*-perfluoro-1-decanol (1.337 g, 2.880 mmol), EDCI (0.552 g, 2.880 mmol), and DMAP (0.075 g, 0.576 mmol) were used. The product was isolated as a colorless viscous oil (1.169 g, η = 70%). R_f (Hex/AcOEt 6:4 (v/v)) = 0.33. ^{1}H NMR ($CDCl_3$) δ_H, ppm: 8.54 (1H, m, N_{py}-C$\underline{H}$-CH, $^3J_{H,H}$ = 4.9 Hz), 7.63 (1H, ddd overlapped, N_{py}-C-CH-C$\underline{H}$, $^3J_{H,H}$ = 7.7 Hz, $^4J_{H,H}$ = 1.8 Hz), 7.25 (1H, d, N_{py}-C-C$\underline{H}$, $^3J_{H,H}$ = 7.7 Hz), 7.17 (1H, m, N_{py}-CH-C$\underline{H}$, $^3J_{H,H}$ = 4.9 Hz, $^3J_{H,H}$ = 7.7 Hz), 4.41 (2H, t, O-C$\underline{H_2}$-CH$_2$, $^3J_{H,H}$ = 6.6 Hz), 3.85 (2H, s, *Py*-C$\underline{H_2}$-C═O), 2.39−2.52 (2H, m, O-CH$_2$-C$\underline{H_2}$). ^{13}C NMR ($CDCl_3$) δ_C, ppm: 170.3 (1C, *Py*-CH$_2$-$\underline{C}$═O), 154.1 (1C, N_{py}-$\underline{C}$-CH), 149.7 (1C, N_{py}-$\underline{C}$H-CH), 136.8 (1C, N_{py}-CH-C-$\underline{C}$H), 123.9 (1C, N_{py}-C-$\underline{C}$H), 122.3 (1C, N_{py}-CH-$\underline{C}$H), 105.3−122.1 (8C, m series, CH$_2$-$\underline{C}$F$_2$-CF$_2$, CH$_2$-CF$_2$-$\underline{C}$F$_2$, CH$_2$-(CF$_2$)$_2$-$\underline{C}$F$_2$, CH$_2$-(CF$_2$)$_3$-$\underline{C}$F$_2$, $\underline{C}$F$_2$-(CF$_2$)$_2$-CF$_3$, $\underline{C}$F$_2$-CF$_2$-CF$_3$, CF$_2$-$\underline{C}$F$_2$-CF$_3$, CF$_2$-CF$_2$-$\underline{C}$F$_3$), 56.9 (1C, t, O-$\underline{C}$H$_2$-CH$_2$, $^3J_{C,F}$ = 4 Hz), 43.8 (1C, *Py*-$\underline{C}$H$_2$-C═O), 30.6 (1C, t, O-CH$_2$-$\underline{C}$H$_2$, $^2J_{C,F}$ = 22 Hz). ^{19}F NMR ($CDCl_3$) δ_F, ppm: −81.05 (3F, t, C$\underline{F_3}$, $^3J_{F,F}$ = 9.6 Hz), −113.78 (2F, m, CH$_2$-C$\underline{F_2}$-CF$_2$), −121.84 (2F, m, CH$_2$-(CF$_2$)$_2$-C$\underline{F_2}$, −122.08 (4F, m, CH$_2$-(CF$_2$)$_3$-C$\underline{F_2}$, CH$_2$-(CF$_2$)$_4$-C$\underline{F_2}$), −122.90 (2F, m, C$\underline{F_2}$-CF$_2$-CF$_3$), −123.72 (2F, m, CH$_2$-CF$_2$-C$\underline{F_2}$), −126.33 (2F, m, C$\underline{F_2}$-CF$_3$).

IR (ν, cm^{-1}): 2970 (CH$_2$), 1742 (C═O), 1594, 1477, 1438, (*Py* C═C, C═N), 1344, 1242−1116 (CF$_2$, CF$_3$), 1199 (C−O). ESI-MS(+): *m*/*z* found 584.25 [M + H]$^+$, calcd for $C_{17}H_{10}F_{17}NO_2$ 583.24. Anal. (%) Calcd for $C_{17}H_{10}F_{17}NO_2$: C 35.01, H 1.73, N 2.40. Found: C 39.21, H 1.48, N 2.62.

1H,1H,2H,2H-Perfluorodecyl-2-(pyridin-3-yl)acetate ***2l.*** 2-(Pyridine-3-yl)acetic acid hydrochloride (0.500 g, 2.880 mmol), TEA (0.400 mL, 2.880 mmol), 1*H*,1*H*,2*H*,2*H*-perfluoro-1-decanol (1.337 g, 2.880 mmol), EDCI (0.552 g, 2.880 mmol), and DMAP (0.075 g, 0.576 mmol, 0.2 equiv) were used. The product was isolated as a white solid (1.902 g, η = 86%); mp (°C) 69.5−70.5. R_f (Hex/AcOEt 5:5 (v/v)) = 0.32.

^{1}H NMR ($CDCl_3$) δ_H, ppm: 8.55 (1H, dd, N_{py}-C$\underline{H}$-CH, $^3J_{H,H}$ = 4.8 Hz, $^4J_{H,H}$ = 1.6 Hz), 8.52 (1H, d, N_{py}-C$\underline{H}$-C, $^4J_{H,H}$ = 1.8 Hz), 7.63 (1H, ddd overlapped, N_{py}-CH-C-C$\underline{H}$, $^3J_{H,H}$ = 7.9 Hz, $^4J_{H,H}$ = 1.6 Hz), 7.28 (1H, dd, N_{py}-CH-C$\underline{H}$, $^3J_{H,H}$ = 4.8 Hz, $^3J_{H,H}$ = 7.9 Hz), 4.42 (2H, t, O-C$\underline{H_2}$-CH$_2$, $^3J_{H,H}$ = 6.5 Hz), 3.66 (2H, s, *Py*-C$\underline{H_2}$-C═O), 2.41−2.53 (2H, m, O-CH$_2$-C$\underline{H_2}$). ^{13}C NMR ($CDCl_3$) δ_C, ppm: 170.4 (1C, CH$_2$-$\underline{C}$═O), 150.5 (1C, N_{py}-$\underline{C}$H-C), 148.9 (1C, N_{py}-$\underline{C}$H-CH), 136.9 (1C, N_{py}-CH-C-$\underline{C}$H), 129.4 (1C, N_{py}-CH-$\underline{C}$-CH), 123.6 (1C, N_{py}-CH-$\underline{C}$H), 104.9−121.9 (8C, m series, CH$_2$-$\underline{C}$F$_2$-CF$_2$, CH$_2$-CF$_2$-$\underline{C}$F$_2$, CH$_2$-(CF$_2$)$_2$-$\underline{C}$F$_2$, CH$_2$-(CF$_2$)$_3$-$\underline{C}$F$_2$, $\underline{C}$F$_2$-(CF$_2$)$_2$-CF$_3$, $\underline{C}$F$_2$-CF$_2$-CF$_3$, CF$_2$-$\underline{C}$F$_2$-CF$_3$, CF$_2$-CF$_2$-$\underline{C}$F$_3$), 57.1 (1C, t, O-$\underline{C}$H$_2$-CH$_2$, $^3J_{C,F}$ = 4 Hz), 38.3 (1C, *Py*-$\underline{C}$H$_2$-C═O), 30.6 (1C, t, O-CH$_2$-$\underline{C}$H$_2$, $^2J_{C,F}$ = 22 Hz).

^{19}F NMR ($CDCl_3$) δ_F, ppm: −80.74 (3F, t, C$\underline{F_3}$, $^3J_{F,F}$ = 9.3 Hz), −113.59 (2F, m, CH$_2$-C$\underline{F_2}$-CF$_2$), −121.64 (2F, m, CH$_2$-(CF$_2$)$_2$-C$\underline{F_2}$), −121.89 (4F, m, CH$_2$-(CF$_2$)$_3$-C$\underline{F_2}$, CH$_2$-(CF$_2$)$_4$-C$\underline{F_2}$), −122.68 (2F, m, C$\underline{F_2}$-CF$_2$-CF$_3$), −123.52 (2F, m, CH$_2$-CF$_2$-C$\underline{F_2}$), −126.08 (2F, m, C$\underline{F_2}$-CF$_3$).

IR (ν, cm^{-1}): 2915 (CH$_2$), 1734 (C═O), 1575, 1482, 1426, 1407 (*Py* C═C, C═N), 1363, 1333, 1245−1115 (CF$_2$, CF$_3$), 1191 (C−O). ESI-MS(+): *m*/*z* found 584.25 [M + H]$^+$, calcd for $C_{17}H_{10}F_{17}NO_2$ 583.24. Anal. (%) Calcd for $C_{17}H_{10}F_{17}NO_2$: C 35.01, H 1.73, N 2.40. Found: C 39.91, H 2.07, N 2.41.

1H,1H,2H,2H-Perfluorodecyl-2-(pyridin-4-yl)acetate ***3l.*** 2-(Pyridine-4-yl)acetic acid hydrochloride (0.500 g, 2.880 mmol), TEA (0.400 mL, 2.880 mmol), 1*H*,1*H*,2*H*,2*H*-perfluoro-1-decanol (1.337 g, 2.880 mmol), EDCI (0.552 g, 2.880 mmol), and DMAP (0.075 g, 0.576 mmol) were used. The product was isolated as a white solid (1.101 g, η = 66%); mp (°C) 76.5−77.5. R_f (Hex/AcOEt 4:6 (v/v)) = 0.33.

^{1}H NMR ($CDCl_3$) δ_H, ppm: 8.55 (2H, d, 2 × N_{py}-C$\underline{H}$-CH, $^3J_{H,H}$ = 4.9 Hz), 7.19 (2H, d, 2 × N_{py}-CH-C$\underline{H}$, $^3J_{H,H}$ = 4.9 Hz), 4.40 (2H, t, O-C$\underline{H_2}$-CH$_2$, $^3J_{H,H}$ = 6.4 Hz), 3.62 (2H, s, *Py*-C$\underline{H_2}$-C═O), 2.38−2.51 (2H, m, O-CH$_2$-C$\underline{H_2}$). ^{13}C NMR ($CDCl_3$) δ_C, ppm: 169.7 (1C, *Py*-CH$_2$-$\underline{C}$═O), 150.2 (2C, 2 × N_{py}-$\underline{C}$H-CH), 142.2 (1C, N_{py}-CH-CH-$\underline{C}$), 124.6 (2C, 2 × N_{py}-CH-$\underline{C}$H), 105.3−121.8 (8C, m series, CH$_2$-$\underline{C}$F$_2$-CF$_2$, CH$_2$-CF$_2$-$\underline{C}$F$_2$, CH$_2$-(CF$_2$)$_2$-$\underline{C}$F$_2$, CH$_2$-(CF$_2$)$_3$-$\underline{C}$F$_2$, $\underline{C}$F$_2$-(CF$_2$)$_2$-CF$_3$, $\underline{C}$F$_2$-CF$_2$-CF$_3$, CF$_2$-$\underline{C}$F$_2$-CF$_3$, CF$_2$-CF$_2$-$\underline{C}$F$_3$), 57.2 (1C, t, O-$\underline{C}$H$_2$-CH$_2$, $^3J_{C,F}$ = 4 Hz), 40.4 (1C, *Py*-$\underline{C}$H$_2$-C═O), 30.5 (1C, t, O-CH$_2$-$\underline{C}$H$_2$, $^2J_{C,F}$ = 22 Hz). ^{19}F NMR ($CDCl_3$) δ_F, ppm: −81.02 (3F, t, C$\underline{F_3}$, $^3J_{F,F}$ = 9.8 Hz), −113.74 (2F, m, CH$_2$-C$\underline{F_2}$-CF$_2$), −121.81 (2F, m, CH$_2$-(CF$_2$)$_2$-C$\underline{F_2}$), −122.07 (4F, m, CH$_2$-(CF$_2$)$_3$-C$\underline{F_2}$, CH$_2$-(CF$_2$)$_4$-C$\underline{F_2}$), −122.88 (2F, m, C$\underline{F_2}$-CF$_2$-CF$_3$), −123.69 (2F, m, CH$_2$-CF$_2$-C$\underline{F_2}$), −126.31 (2F, m, C$\underline{F_2}$-CF$_3$).

IR (ν, cm^{-1}): 2915 (CH$_2$), 1738 (C═O), 1606, 1560, 1421, (*Py* C═C, C═N), 1361, 1330, 1116−1241 (CF$_2$, CF$_3$), 1194 (C−O). ESI-MS(+): *m*/*z* found 584.25 [M + H]$^+$, calcd for $C_{17}H_{10}F_{17}NO_2$ 583.24. Anal. (%) Calcd for $C_{17}H_{10}F_{17}NO_2$: C 35.01, H 1.73, N 2.40. Found: C 35.10, H 1.57, N 2.41.

General Procedure for the Synthesis of the [Ru(η^6-*p*-cymene)Cl$_2$X] Complexes (with X = 1l−3l) 6−8. To a solution of [Ru(η^6-*p*-cymene)Cl$_2$]$_2$ (1 equiv) in CH_2Cl_2 (10 mL), a solution of the corresponding ester ligand **1l**−**3l** (2.1 equiv) was added, and the resulting mixture was stirred at rt in the dark for about 4 days. The reaction mixture was concentrated under reduced pressure almost to dryness, and the product was precipitated with Et_2O. The precipitate was washed with Et_2O (3 × 20 mL), hexane (20 mL), and again Et_2O (20 mL) and then removed by filtration and dried under a flow of N_2.

[Ru(η^6-p-cymene)Cl$_2$(1H,1H,2H,2H -perfluorodecyl-2-(pyridin-2-yl)acetate)] ***6.*** [Ru(η^6-*p*-cymene)Cl$_2$]$_2$ (0.185 g, 0.302 mmol) and 1*H*,1*H*,2*H*,2*H*-perfluorodecyl-2-(pyridin-2-yl)acetate (**1l**) (0.440 g, 0.754 mmol) were used. The product was isolated as an orange solid (0.385 g, η = 72%); mp (°C) 221−223 (decomp).

^{1}H NMR ($CDCl_3$, 318 K) δ_H, ppm: 8.59 (1H, m br, N_{py}-C$\underline{H}$-CH), 7.66 (1H, ddd overlapped, N_{py}-C-CH-C$\underline{H}$, $^3J_{H,H}$ = 7.7 Hz, $^4J_{H,H}$ = 1.4 Hz), 7.28 (1H, d, N_{py}-C-C$\underline{H}$, $^3J_{H,H}$ = 7.7 Hz), 7.19 (1H, dd, N_{py}-CH-C$\underline{H}$, $^3J_{H,H}$ = 7.7 Hz, $^3J_{H,H}$ = 4.9 Hz), 5.47 (2H, d, 2 × CH$_3$-C-CH-C$\underline{H}$(*Ar*), $^3J_{H,H}$ = 5.8 Hz), 5.33 (2H, d, 2 × CH$_3$-C-C$\underline{H}$(*Ar*), $^3J_{H,H}$ = 5.8 Hz), 4.44 (2H, t, O-C$\underline{H_2}$-CH$_2$, $^3J_{H,H}$ = 6.6 Hz), 3.90 (2H, s br, *Py*-C$\underline{H_2}$-C═O), 2.93 (1H, sept, *Ar*-C$\underline{H}$(CH$_3$)$_2$, $^3J_{H,H}$ = 6.9 Hz), 2.42−2.55 (2H, m, O-CH$_2$-C$\underline{H_2}$), 2.16 (3H, s, *Ar*-C$\underline{H_3}$), 1.28 (6H, d, *Ar*-CH(C$\underline{H_3}$)$_2$, $^3J_{H,H}$ = 6.9 Hz).

^{13}C NMR ($CDCl_3$, 318 K) δ_C, ppm: 170.3 (1C, CH$_2$-$\underline{C}$═O), 154.4 (1C, br, N_{py}-$\underline{C}$-CH), 150.1 (1C, br, N_{py}-$\underline{C}$H-CH), 136.9 (1C, N_{py}-C-CH-$\underline{C}$H), 124.1 (1C, N_{py}-C-$\underline{C}$H), 122.4 (1C, N_{py}-CH-$\underline{C}$H), 107.2−120.8 (8C, m series, CH$_2$-$\underline{C}$F$_2$-CF$_2$, CH$_2$-CF$_2$-$\underline{C}$F$_2$, CH$_2$-(CF$_2$)$_2$-$\underline{C}$F$_2$, CH$_2$-(CF$_2$)$_3$-$\underline{C}$F$_2$, $\underline{C}$F$_2$-(CF$_2$)$_2$-CF$_3$, $\underline{C}$F$_2$-CF$_2$-CF$_3$, CF$_2$-$\underline{C}$F$_2$-CF$_3$, CF$_2$-CF$_2$-$\underline{C}$F$_3$), 101.5 (1C, CH$_3$-C-CH-CH-$\underline{C}$(*Ar*)), 96.9 (1C, CH$_3$-$\underline{C}$-CH(*Ar*)), 81.5 (2C, 2 × CH$_3$-C-CH-$\underline{C}$H(*Ar*)), 80.8 (2C, 2 × CH$_3$-C-$\underline{C}$H(*Ar*)), 57.0 (1C, t, O-$\underline{C}$H$_2$-CH$_2$, $^3J_{C,F}$ = 5 Hz), 44.0 (1C, *Py*-$\underline{C}$H$_2$-C═O), 30.9 (1C, t, O-CH$_2$-$\underline{C}$H$_2$, $^2J_{C,F}$ = 22 Hz), 30.8 (1C, *Ar*-$\underline{C}$H(CH$_3$)$_2$), 22.3 (2C, *Ar*-CH(C$\underline{H_3}$)$_2$), 19.0 (1C, *Ar*-$\underline{C}$H$_3$).

^{19}F NMR ($CDCl_3$) δ_F, ppm: −80.73 (3F, t, C$\underline{F_3}$, $^3J_{F,F}$ = 9.8 Hz), −113.58 (2F, m, CH$_2$-C$\underline{F_2}$-CF$_2$), −121.65 (2F, m, CH$_2$-(CF$_2$)$_2$-C$\underline{F_2}$), −121.89 (4F, m, CH$_2$-(CF$_2$)$_3$-C$\underline{F_2}$, CH$_2$-(CF$_2$)$_4$-C$\underline{F_2}$), −122.68 (2F, m, C$\underline{F_2}$-CF$_2$-CF$_3$), −123.53 (2F, m, CH$_2$-CF$_2$-C$\underline{F_2}$), −126.06 (2F, m, C$\underline{F_2}$-CF$_3$).

IR (ν, cm^{-1}): 3061 (CH-*Ar*), 2961, 2867 (CH$_2$, CH, CH$_3$), 1742 (C═O), 1567, 1541, 1436 (*Py* C═C, C═N), 1362, 1314, 1117−

dx.doi.org/10.1021/jm5002748 | *J. Med. Chem.* 2014, 57, 3546−3558

1239 (CF_2, CF_3), 1195 (C−O). ESI-MS(+): *m/z* found 854.04 $[M - Cl]^+$, calcd for $C_{27}H_{24}ClF_{17}NO_2Ru$ 854.03, the experimental isotopic pattern fits well the calculated one. Anal. (%) Calcd for $C_{27}H_{24}Cl_2F_{17}NO_2Ru$: C 36.46, H 2.72, N 1.57. Found: C 36.41, H 2.67, N 1.53.

[Ru(η^6-p-cymene)Cl$_2$(1H,1H,2H,2H-perfluorodecyl-2-(pyridin-3-yl)acetate)] **7**. $[Ru(\eta^6\text{-}p\text{-cymene})Cl_2]_2$ (0.220 g, 0.359 mmol), 1*H*,1*H*,2*H*,2*H*-perfluorodecyl-2-(pyridin-3-yl)acetate (**2l**) (0.440 g, 0.754 mmol) were used. The product was isolated as an orange solid (0.579 g, η = 91%); mp (°C) 158.2−160.

^{1}H NMR ($CDCl_3$) δ_H, ppm: 8.97 (1H, d, N_{py}-C*H*-CH, $^3J_{H,H}$ = 5.6 Hz), 8.96 (1H, s, N_{py}-C*H*-C), 7.65 (1H, d, N_{py}-CH-C-C*H*, $^3J_{H,H}$ = 7.8 Hz), 7.28 (1H, dd overlapped, N_{py}-CH-C*H*, $^3J_{H,H}$ = 5.6 Hz, $^3J_{H,H}$ = 7.8 Hz), 5.45 (2H, d, 2 × CH_3-C-CH-C*H*(*Ar*), $^3J_{H,H}$ = 5.9 Hz), 5.21 (2H, d, 2 × CH_3-C-C*H*-(*Ar*), $^3J_{H,H}$ = 5.9 Hz), 4.44 (2H, t, O-C*H*$_2$-CH_2, $^3J_{H,H}$ = 6.5 Hz), 3.67 (2H, s, *Py*-C*H*$_2$-C═O), 2.96−3.05 (1H, sept, *Ar*-C*H*(CH_3)$_2$, $^3J_{H,H}$ = 6.9 Hz), 2.46−2.58 (2H, m, O-CH_2-C*H*$_2$), 2.07 (3H, s, *Ar*-C*H*$_3$), 1.30 (6H, d, *Ar*-CH(C*H*$_3$)$_2$, $^3J_{H,H}$ = 6.9 Hz).

^{13}C NMR ($CDCl_3$) δ_C, ppm: 169.9 (1C, CH_2-*C*═O), 155.6 (1C, N_{py}-*C*H-C), 153.6 (1C, N_{py}-*C*H-CH), 138.8 (1C, N_{py}-CH-C-*C*H), 130.4 (1C, N_{py}-CH-*C*-CH), 124.2 (1C, N_{py}-CH-*C*H), 105.2−121.8 (8C, m series, CH_2-*C*F_2-CF_2, CH_2-CF_2-*C*F_2, CH_2-$(CF_2)_2$-*C*F_2, CH_2-$(CF_2)_3$-*C*F_2, *C*F_2-$(CF_2)_2$-CF_3, *C*F_2-CF_2-CF_3, CF_2-*C*F_2-CF_3, CF_2-CF_2-*C*F_3), 103.5 (1C, CH_3-C-CH-CH-*C*(*Ar*)), 97.4 (1C, CH_3-*C*-CH(*Ar*)), 83.1 (2C, 2 × CH_3-C-CH-*C*H(*Ar*)), 82.2 (2C, 2 × CH_3-C-*C*H(*Ar*)), 57.3 (1C, m, O-*C*H_2-CH_2, $^3J_{C,F}$ = 4 Hz), 37.7 (1C, *Py*-*C*H_2-C═O), 30.7 (1C, *Ar*-*C*H(CH_3)$_2$), 30.5 (1C, t, O-CH_2-*C*H_2, $^2J_{C,F}$ = 22 Hz), 22.3 (2C, *Ar*-CH(*C*H_3)$_2$), 18.1 (1C, *Ar*-*C*H_3).

^{19}F NMR ($CDCl_3$) δ_F, ppm: −80.72 (3F, t, C*F*$_3$, $^3J_{F,F}$ = 9.8 Hz), −113.59 (2F, m, CH_2-C*F*$_2$-CF_2), −121.59 (2F, m, CH_2-$(CF_2)_2$-C*F*$_2$), −121.85 (4F, m, CH_2-$(CF_2)_3$-C*F*$_2$, CH_2-$(CF_2)_4$-C*F*$_2$), −122.66 (2F, m, C*F*$_2$-CF_2-CF_3), −123.45 (2F, m, CH_2-CF_2-C*F*$_2$), −126.06 (2F, m, C*F*$_2$-CF_3).

IR (ν, cm^{-1}): 3042 (CH-*Ar*), 2960, 2868 (CH_2, CH, CH_3), 1741 (C═O), 1572, 1503, 1431 (*Py* C═C, C═N), 1353, 1330, 1113−1232 (CF_2, CF_3), 1199 (C−O). ESI-MS(+): *m/z* found 853.92 $[M - Cl]^+$, calcd for $C_{27}H_{24}ClF_{17}NO_2Ru$ 854.03, the experimental isotopic pattern fits well the calculated one. Anal. (%) Calcd for $C_{27}H_{24}Cl_2F_{17}NO_2Ru$: C 36.46, H 2.72, N 1.57. Found: C 36.69, H 2.73, N 1.53.

[Ru(η^6-p-cymene)Cl$_2$(1H,1H,2H,2H-perfluorodecyl-2-(pyridin-4-yl)acetate)] **8**. $[Ru(\eta^6\text{-}p\text{-cymene})Cl_2]_2$ (0.220 g, 0.359 mmol) and 1*H*,1*H*,2*H*,2*H*-perfluorodecyl-2-(pyridin-4-yl)acetate (**3l**) (0.440 g, 0.754 mmol) were used. The product was isolated as an orange solid (0.544 g, η = 85%); mp (°C) 156.5−157.5.

^{1}H NMR ($CDCl_3$) δ_H, ppm: 8.97 (2H, d, 2 × N_{py}-C*H*-CH, $^3J_{H,H}$ = 6.4 Hz), 7.23 (2H, d, 2 × N_{py}-CH-C*H*, $^3J_{H,H}$ = 6.4 Hz), 5.42 (2H, d, 2 × CH_3-C-CH-C*H*(*Ar*), $^3J_{H,H}$ = 5.9 Hz), 5.21 (2H, d, 2 × CH_3-C-C*H*(*Ar*), $^3J_{H,H}$ = 5.9 Hz), 4.43 (2H, t, O-C*H*$_2$-CH_2, $^3J_{H,H}$ = 6.3 Hz), 3.69 (2H, s, *Py*-C*H*$_2$-C═O), 2.97−3.04 (1H, sept, *Ar*-C*H*(CH_3)$_2$, $^3J_{H,H}$ = 6.9 Hz), 2.43−2.55 (2H, m, O-CH_2-C*H*$_2$), 2.10 (3H, s, *Ar*-C*H*$_3$), 1.30 (6H, d, *Ar*-CH(C*H*$_3$)$_2$, $^3J_{H,H}$ = 6.9 Hz).

^{13}C NMR ($CDCl_3$) δ_C, ppm: 169.0 (1C, CH_2-*C*═O), 154.7 (2C, 2 × N_{py}-*C*H-CH), 144.6 (1C, N_{py}-CH-CH-*C*), 125.5 (2C, 2 × N_{py}-CH-*C*H), 105.5−121.4 (8C, m series, CH_2-*C*F_2-CF_2, CH_2-CF_2-*C*F_2, CH_2-$(CF_2)_2$-*C*F_2, CH_2-$(CF_2)_3$-*C*F_2, *C*F_2-$(CF_2)_2$-CF_3, *C*F_2-CF_2-CF_3, CF_2-*C*F_2-CF_3, CF_2-CF_2-*C*F_3), 103.6 (1C, CH_3-C-CH-CH-*C*(*Ar*)), 97.1 (1C, CH_3-*C*-CH(*Ar*)), 82.7 (2C, 2 × CH_3-C-CH-*C*H(*Ar*)), 82.3 (2C, 2 × CH_3-C-*C*H(*Ar*)), 57.3 (1C, t, O-*C*H_2-CH_2, $^3J_{C,F}$ = 4 Hz), 39.8 (1C, *Py*-*C*H_2-C═O), 30.7 (1C, *Ar*-*C*H(CH_3)$_2$), 30.4 (1C, t, O-CH_2-*C*H_2, $^2J_{C,F}$ = 22 Hz), 22.2 (2C, *Ar*-CH(*C*H_3)$_2$), 18.2 (1C, *Ar*-*C*H_3).

^{19}F NMR ($CDCl_3$) δ_F, ppm: −80.72 (3F, t, C*F*$_3$, $^3J_{F,F}$ = 9.8 Hz), −113.57 (2F, m, CH_2-C*F*$_2$-CF_2), −121.60 (2F, m, CH_2-$(CF_2)_2$-C*F*$_2$), −121.86 (4F, m, CH_2-$(CF_2)_3$-C*F*$_2$, CH_2-$(CF_2)_4$-C*F*$_2$), −122.67 (2F, m, C*F*$_2$-CF_2-CF_3), −123.49 (2F, m, CH_2-CF_2-C*F*$_2$), −126.07 (2F, m, C*F*$_2$-CF_3).

IR (ν, cm^{-1}): 3058 (CH-*Ar*), 2963, 2873 (CH_2, CH, CH_3), 1732 (C═O), 1502, 1472, 1426 (*Py* C═C, C═N), 1351, 1321, 1236−1117 (CF_2, CF_3), 1224 (C−O). ESI-MS(+): *m/z* found 854.03 $[M - Cl]^+$, calcd for $C_{27}H_{24}ClF_{17}NO_2Ru$ 854.03, the experimental isotopic pattern fits well the calculated one. Anal. (%) Calcd for $C_{27}H_{24}Cl_2F_{17}NO_2Ru$: C 36.46, H 2.72, N 1.57. Found: C 36.37, H 2.77, N 1.58.

Synthesis of 2-(Benzyloxy)-2-oxoethyl-3-(pyridin-3-yl)-propanoate (step a before 4l). To a suspension of 3-(pyridin-3-yl)propanoic acid (1 equiv, 0.800 g, 5.292 mmol) in dry CH_2Cl_2 (50 mL), EDCI (1 equiv, 1.014 g, 5.292 mmol) was added, and the resulting mixture was stirred at rt for 15 min. Then benzyl-2-hydroxyacetate (1 equiv, 0.751 mL, 5.292 mmol) and DMAP (0.2 equiv, 0.137 g, 1.058 mmol) were added, and the solution was stirred at rt for about 2 days. The mixture was then diluted with CH_2Cl_2 (200 mL), washed with H_2O (150 mL), the aqueous phase re-extracted with CH_2Cl_2 (2 × 100 mL), and the combined organic phases washed with brine (200 mL), dried over anhydrous Na_2SO_4, and concentrated under reduced pressure. Solid deposition on Celite and purification by flash chromatography afforded the product as a colorless oil (1.365 g, η = 86%). R_f (Hex/AcOEt 3:7 (v/v)) = 0.28.

^{1}H NMR ($CDCl_3$) δ_H, ppm: 8.49 (1H, d, N_{py}-C*H*-C, $^4J_{H,H}$ = 1.7 Hz), 8.47 (1H, dd, N_{py}-C*H*-CH, $^3J_{H,H}$ = 4.8 Hz, $^4J_{H,H}$ = 1.6 Hz), 7.54 (1H, ddd overlapped, N_{py}-CH-C-C*H*, $^3J_{H,H}$ = 7.7 Hz, $^4J_{H,H}$ = 1.7 Hz), 7.32−7.39 (5H, m, 5 × C*H*(*Ph*)), 7.22 (1H, dd, N_{py}-CH-C*H*, $^3J_{H,H}$ = 4.8 Hz, $^4J_{d,c}$ = 7.7 Hz), 5.19 (2H, s, O-C*H*$_2$-Ph), 4.66 (2H, s, O-C*H*$_2$-C═O), 2.99 (2H, t, *Py*-C*H*$_2$-CH_2-C═O, $^3J_{H,H}$ = 7.8 Hz), 2.75 (2H, t, *Py*-CH_2-C*H*$_2$-C═O, $^3J_{H,H}$ = 7.8 Hz).

^{13}C NMR ($CDCl_3$) δ_C, ppm: 171.8 (1C, CH_2-CH_2-*C*═O), 167.6 (1C, O-CH_2-*C*═O), 149.9 (1C, N_{py}-*C*H-C), 148.0 (1C, N_{py}-*C*H-CH), 135.9 (1C, N_{py}-CH-C-*C*H), 135.6 (1C, N_{py}-CH-*C*-CH), 135.1 (1C, CH_2-*C*-CH(*Ar*)), 128.8 (2C, 2 × CH_2-C-CH-*C*H(*Ar*)), 128.7 (1C, CH_2-C-CH-CH-*C*H(*Ar*)), 128.5 (2C, 2 × CH_2-C-*C*H-CH(*Ar*)), 123.5 (1C, C-d), N_{py}-CH-*C*H, 67.3 (1C, O-*C*H_2−Ph), 60.9 (1C, O-*C*H_2-C═O), 34.9 (1C, *Py*-CH_2-*C*H_2-C═O), 27.9 (1C, *Py*-*C*H_2-CH_2-C═O).

IR (ν, cm^{-1}): 3031 (CH-*Ar*), 2957 (CH_2), 1763 (C═O), 1742 (C═O), 1575, 1497, 1480, 1456, 1422 (*Py* C═C, C═N), 1222 (C−O). ESI-MS(+): *m/z* found 300.11 $[M + H]^+$, calcd for $C_{17}H_{17}NO_4$ 299.32. Anal. (%) Calcd for $C_{17}H_{17}NO_4$: C 68.21, H 5.72, N 4.68. Found: C 69.33, H 5.80, N 4.72.

Synthesis of 2-((3-(Pyridin-3-yl)propanoyl)oxy)acetic Acid (step b before 4l). To a solution of 2-(benzyloxy)-2-oxoethyl-3-(pyridin-3-yl)propanoate (1.100 g, 3.645 mmol, 1 equiv) in MeOH (150 mL), Pd/C (10%) (0.05 equiv) was added, and the resulting suspension was degassed for further 15 min. Then H_2 gas was passed through the reaction mixture for 8 h and the mixture stirred under a H_2 atmosphere overnight. The mixture was filtrated on a Celite pad which was further washed with CH_2Cl_2/MeOH 50:50 mixture (5 × 60 mL). The filtrate evaporated to dryness, and the resulting solid purified by flash chromatography to afford a white solid (0.344 g, η = 45%); mp (°C) 126.5−128. R_f (CH_2Cl_2/MeOH 8:2 (v/v)) = 0.44.

^{1}H NMR (MeOD-d^4) δ_H, ppm: 8.52 (1H, s, N_{py}-C*H*-C), 8.43 (1H, dd overlapped, N_{py}-C*H*-CH, $^3J_{H,H}$ = 5 Hz), 7.86 (1H, ddd overlapped, N_{py}-CH-C-C*H*, $^3J_{H,H}$ = 7.8 Hz), 7.45 (1H, dd, N_{py}-CH-C*H*, $^3J_{H,H}$ = 5 Hz, $^4J_{H,H}$ = 7.8 Hz), 4.60 (2H, s, O-C*H*$_2$-C═O), 3.06 (2H, t, *Py*-C*H*$_2$-CH_2-C═O, $^3J_{H,H}$ = 7.3 Hz), 2.83 (2H, t, *Py*-CH_2-C*H*$_2$-C═O; $^3J_{H,H}$ = 7.3 Hz).

^{13}C NMR (MeOD-d^4) δ_C, ppm: 173.5 (1C, CH_2-CH_2-*C*═O), 172.6 (1C, O-CH_2-*C*═O), 149.3 (1C, N_{py}-*C*H-C), 147.0 (1C, N_{py}-*C*H-CH), 139.6 (1C, N_{py}-CH-C-*C*H), 139.0 (1C, N_{py}-CH-*C*-CH), 125.5 (1C, N_{py}-CH-*C*H), 62.3 (1C, O-*C*H_2-C═O), 35.5 (1C, *Py*-CH_2-*C*H_2-C═O), 28.7 (1C, *Py*-*C*H_2-CH_2-C═O).

IR (ν, cm^{-1}): 2924 (CH_2), 2360 (O−H), 1719 (C═O), 1583, 1479 (C═C, C═N), 1254 (C−O). ESI-MS(+): *m/z* found 210.05 $[M + H]^+$, calcd for $C_{10}H_{11}NO_4$ 209.20. Anal. (%) Calcd for $C_{10}H_{11}NO_4$: C 57.41, H 5.30, N 6.70. Found: C 57.27, H 5.45, N 6.62.

Synthesis of 2-((1*H*,1*H*,2*H*,2*H*-Perfluorodecyl)oxy)-2-oxoethyl-3-(pyridin-3-yl)propanoate 4l. To a suspension of 2-((3-(pyridin-3-yl)propanoyl)oxy)acetic acid (0.344 g, 1.644 mmol, 1 equiv) in CH_2Cl_2 (75 mL), EDCI (0.315 g, 1.644 mmol,1 equiv) was added and the mixture was stirred at rt for 15 min. Next, 1*H*,1*H*,2*H*,2*H*-perfluoro-1-decanol (0.763 g, 1.644 mmol, 1 equiv) and DMAP (0.043 g, 0.329 mmol, 0.2 equiv) were added, and the

dx.doi.org/10.1021/jm5002748 | J. Med. Chem. 2014, 57, 3546−3558

resulting mixture was stirred at rt for about 4 days. The mixture was then diluted with CH_2Cl_2 (100 mL), washed with H_2O (100 mL), the aqueous phase re-extracted with CH_2Cl_2 (2 × 100 mL), and the combined organic phases were washed with brine (150 mL), dried over anhydrous Na_2SO_4, and concentrated under reduced pressure. Deposition of the solid on Celite and purification by flash chromatography afford the product as a colorless viscous oil (0.614 g, η = 57%). R_f (Hex/AcOEt 4:6 (v/v)) = 0.35.

^{1}H NMR ($CDCl_3$) δ_H, ppm: 8.48 (1H, d, N_{py}-C$\underline{H}$-C, $^4J_{H,H}$ = 2.1 Hz), 8.45 (1H, dd, N_{py}-C$\underline{H}$-CH, $^3J_{H,H}$ = 4.8 Hz, $^4J_{H,H}$ = 1.7 Hz), 7.52 (1H, ddd overlapped, N_{py}-CH-C-C$\underline{H}$, $^3J_{H,H}$ = 7.8 Hz, $^4J_{H,H}$ = 1.7 Hz), 7.20 (1H, dd, N_{py}-CH-C$\underline{H}$, $^3J_{H,H}$ = 4.8 Hz, $^4J_{H,H}$ = 7.8 Hz), 4.61 (2H, s, O-C$\underline{H_2}$-C=O), 4.45 (2H, t, O-C$\underline{H_2}$-CH$_2$, $^3J_{H,H}$ = 6.5 Hz), 2.98 (2H, t, *Py*-C$\underline{H_2}$-CH$_2$-C=O, $^3J_{H,H}$ = 7.6 Hz), 2.75 (2H, t, *Py*-CH$_2$-C$\underline{H_2}$-C=O, $^3J_{H,H}$ = 7.6 Hz), 2.40−2.53 (2H, m, O-CH$_2$-C$\underline{H_2}$).

^{13}C NMR ($CDCl_3$) δ_C, ppm: 171.8 (1C, CH$_2$-CH$_2$-$\underline{C}$=O), 167.4 (1C, O-CH$_2$-$\underline{C}$=O), 150.0 (1C, N_{py}-$\underline{C}$H-C), 148.1 (1C, N_{py}-$\underline{C}$H-CH), 135.9 (1C, N_{py}-CH-C-$\underline{C}$H), 135.6 (1C, N_{py}-CH-$\underline{C}$-CH), 123.5 (1C, N_{py}-CH-$\underline{C}$H), 105.3−121.9 (8C, m series, CH$_2$-$\underline{C}$F$_2$-CF$_2$, CH$_2$-CF$_2$-$\underline{C}$F$_2$, CH$_2$-(CF$_2$)$_2$-$\underline{C}$F$_2$, CH$_2$-(CF$_2$)$_3$-$\underline{C}$F$_2$, $\underline{C}$F$_2$-(CF$_2$)$_2$-CF$_3$, $\underline{C}$F$_2$-CF$_2$-CF$_3$, CF$_2$-$\underline{C}$F$_2$-CF$_3$, CF$_2$-CF$_2$-$\underline{C}$F$_3$), 60.7 (1C, O-$\underline{C}$H$_2$-C=O), 57.3 (1C, t, O-$\underline{C}$H$_2$-CH$_2$, $^3J_{C,F}$ = 4 Hz), 34.9 (1C, *Py*-CH$_2$-$\underline{C}$H$_2$-C=O), 30.6 (1C, t, O-CH$_2$-$\underline{C}$H$_2$, $^2J_{C,F}$ = 22 Hz), 27.9 (1C, *Py*-$\underline{C}$H$_2$-CH$_2$-C=O).

^{19}F NMR ($CDCl_3$) δ_F, ppm: −80.76 (3F, t, C$\underline{F_3}$, $^3J_{F,F}$ = 9.8 Hz), −113.64 (2F, m, CH$_2$-C$\underline{F_2}$-CF$_2$), −121.65 (2F, m, CH$_2$-(CF$_2$)$_2$-C$\underline{F_2}$), −121.88 (4F, m, CH$_2$-(CF$_2$)$_3$-C$\underline{F_2}$, CH$_2$-(CF$_2$)$_4$-C$\underline{F_2}$), −122.60 (2F, m, C$\underline{F_2}$-CF$_2$-CF$_3$), −123.48 (2F, m, CH$_2$-CF$_2$-C$\underline{F_2}$), −126.07 (2F, m, C$\underline{F_2}$-CF$_3$).

IR (ν, cm^{-1}): 2956 (CH$_2$), 1746 (C=O), 1576, 1480, 1425 (*Py* C=C, C=N), 1370, 1331, 1246−1116 (CF$_2$, CF$_3$), 1197 (C−O). ESI-MS(+): *m*/*z* found 656.07 [M + H]$^+$, calcd for $C_{20}H_{14}F_{17}NO_4$ 655.30. Anal. (%) Calcd for $C_{20}H_{14}F_{17}NO_4$: C 36.66, H 2.15, N 2.14. Found: C 36.66, H 2.16, N 2.11.

Synthesis of [Ru(η^6-*p*-cymene)Cl$_2$(2-((1*H*,1*H*,2*H*,2*H*-perfluorodecyl)oxy)-2-oxoethyl-3-(pyridin-3-yl)propanoate)] 9. To a solution of [Ru(η^6-*p*-cymene)Cl$_2$]$_2$ (0.165 g, 0.269 mmol, 1 equiv) in CH_2Cl_2 (10 mL), a solution of 2-((1*H*,1*H*,2*H*,2*H*-perfluorodecyl)oxy)-2-oxoethyl-3-(pyridin-3-yl)propanoate (**4l**) (0.370 g, 0.565 mmol, 2.1 equiv) in CH_2Cl_2 (20 mL) was added, and the resulting mixture was stirred at rt in the dark for about 4 days. The reaction mixture was concentrated under reduced pressure almost to dryness, and the obtained viscous orange oil was washed with Et_2O (3 × 20 mL), hexane (20 mL), and again Et_2O (20 mL). The resulting orange oil was dried under high vacuum to afford an orange solid (0.514 g, η = 97%); mp (°C) = 89.5−91.

^{1}H NMR ($CDCl_3$) δ_H, ppm: 8.93 (1H, s, N_{py}-C$\underline{H}$-C), 8.89 (1H, d, N_{py}-C$\underline{H}$-CH, $^3J_{H,H}$ = 4.3 Hz), 7.61 (1H, d, N_{py}-CH-C-C$\underline{H}$, $^3J_{H,H}$ = 6.5 Hz), 7.22 (1H, m, N_{py}-CH-C$\underline{H}$), 5.43 (2H, d, 2 × CH$_3$-C-CH-C$\underline{H}$(*Ar*), $^3J_{H,H}$ = 4.9 Hz), 5.21 (2H, d, 2 × CH$_3$-C-C$\underline{H}$(*Ar*), $^3J_{H,H}$ = 4.9 Hz), 4.63 (2H, s, O-C$\underline{H_2}$-C=O), 4.46 (2H, t, O-C$\underline{H_2}$-CH$_2$, $^3J_{H,H}$ = 6.3 Hz), 2.96−3.01 (1H, m, *Ar*-C$\underline{H}$(CH$_3$)$_2$), 3.01 (2H, t, *Py*-C$\underline{H_2}$-CH$_2$-C=O, $^3J_{H,H}$ = 6.5 Hz), 2.78 (2H, t, *Py*-CH$_2$-C$\underline{H_2}$-C=O, $^3J_{H,H}$ = 6.5 Hz), 2.43−2.54 (2H, m, O-CH$_2$-C$\underline{H_2}$), 2.08 (3H, s, *Ar*-C$\underline{H_3}$), 1.31 (6H, d, *Ar*-CH(C$\underline{H_3}$)$_2$, $^3J_{H,H}$ = 7.1 Hz).

^{13}C NMR ($CDCl_3$) δ_C, ppm: 171.5 (1C, CH$_2$-CH$_2$-$\underline{C}$=O), 167.4 (1C, O-CH$_2$-$\underline{C}$=O), 155.1 (1C, N_{py}-$\underline{C}$H-C), 153.0 (1C, N_{py}-$\underline{C}$H-CH), 137.8 (1C, N_{py}-CH-C-$\underline{C}$H), 136.8 (1C, N_{py}-CH-$\underline{C}$-CH), 124.3 (1C, N_{py}-CH-$\underline{C}$H), 105.3−121.9 (8C, m series, CH$_2$-$\underline{C}$F$_2$-CF$_2$, CH$_2$-CF$_2$-$\underline{C}$F$_2$, CH$_2$-(CF$_2$)$_2$-$\underline{C}$F$_2$, CH$_2$-(CF$_2$)$_3$-$\underline{C}$F$_2$, $\underline{C}$F$_2$-(CF$_2$)$_2$-CF$_3$, $\underline{C}$F$_2$-CF$_2$-CF$_3$, CF$_2$-$\underline{C}$F$_2$-CF$_3$, CF$_2$-CF$_2$-$\underline{C}$F$_3$), 103.5 (1C, CH$_3$-C-CH-CH-$\underline{C}$(*Ar*)), 97.3 (1C, CH$_3$-$\underline{C}$-CH(*Ar*)), 82.8 (2C, 2 × CH$_3$-C-CH-$\underline{C}$H(*Ar*)), 82.3 (2C, 2 × CH$_3$-C-$\underline{C}$H(*Ar*)), 60.7 (1C, O-$\underline{C}$H$_2$-C=O), 57.3 (1C, t, O-$\underline{C}$H$_2$-CH$_2$, $^3J_{C,F}$ = 4 Hz), 34.4 (1C, *Py*-CH$_2$-$\underline{C}$H$_2$-C=O), 30.7 (1C, *Ar*-$\underline{C}$H(CH$_3$)$_2$), 30.5 (1C, t, O-CH$_2$-$\underline{C}$H$_2$, $^2J_{C,F}$ = 22 Hz), 27.7 (1C, *Py*-$\underline{C}$H$_2$-CH$_2$-C=O), 22.4 (2C, *Ar*-CH(C$\underline{H_3}$)$_2$), 18.2 (1C, *Ar*-$\underline{C}$H$_3$).

^{19}F NMR ($CDCl_3$) δ_F, ppm: −80.72 (3F, t, C$\underline{F_3}$, $^3J_{F,F}$ = 9.3 Hz), −113.59 (2F, m, CH$_2$-C$\underline{F_2}$-CF$_2$), −121.62 (2F, m, CH$_2$-(CF$_2$)$_2$-C$\underline{F_2}$), −121.88 (4F, m, CH$_2$-(CF$_2$)$_3$-C$\underline{F_2}$, CH$_2$-(CF$_2$)$_4$-C$\underline{F_2}$), −122.68 (2F, m, C$\underline{F_2}$-CF$_2$-CF$_3$), −123.46 (2F, m, CH$_2$-CF$_2$-C$\underline{F_2}$), −126.07 (2F, m, C$\underline{F_2}$-CF$_3$).

IR (ν, cm^{-1}): 3052 (CH-*Ar*), 2958−2872 (CH$_2$, CH, CH$_3$), 1744 (C=O), 1473, 1425 (C=C, C=N), 1384, 1331, 1115−1234 (CF$_2$, CF$_3$), 1198 (C−O). ESI-MS(+): *m*/*z* found 925.92 [M − Cl]$^+$, calcd for $C_{30}H_{28}ClF_{17}NO_4Ru$ 926.05, the experimental isotopic pattern fits well the calculated one. Anal. (%) Calcd for $C_{30}H_{28}C_{12}F_{17}NO_4Ru$: C 37.48, H 2.94, N 1.46. Found: C 37.49, H 2.99, N 1.46.

X-ray Diffraction. The diffraction data for compound **2** were measured at low temperature [140(2) K] using Mo Kα radiation on a mar345dtb system in combination with a Genix Hi-Flux small focus generator (*mar*μ*X* system). The data reduction was carried out by *automar*.[52] The solution and refinement were performed by SHELX.[53] The structure was refined using full-matrix least-squares based on F^2 with all non-hydrogen atoms anisotropically defined. Hydrogen atoms were placed in calculated positions by means of the "riding" model.

Cell Culture. Human A2780 and A2780cisR ovarian carcinoma cells were obtained from the European Centre of Cell Cultures (ECACC, UK). Adenocarcinomic human alveolar basal epithelial cells (A549), human breast adenocarcinoma cells (MDA-MB-231 and MCF7), and nontumorigenic HEK-293 cells were provided by the Institute of Pathology, CHUV, Lausanne, Switzerland. A2780, A2780cisR, and A549 cells were routinely grown in RPMI 1640 medium supplemented with GlutaMAX (Gibco), while MDA-MB-231, MCF-7, and HEK-293 were grown in DMEM medium, both containing heat-inactivated fetal calf serum (FCS, Sigma, USA) (10%) and antibiotics (penicillin/streptomycin) at 37 °C and CO_2 (5%).

Cell Proliferation Inhibition. Cytotoxicity was determined using the MTT assay (MTT = 3-(4,5-dimethyl-2-thiazolyl)-2,5-diphenyl-2*H*-tetrazolium bromide). Cells were seeded in 96-well plates as monolayers with 100 μL of cell solution (approximately 20000 cells) per well and preincubated for 24 h in medium supplemented with 10% FCS. Compounds were prepared as DMSO solution that were rapidly dissolved in the culture medium and serially diluted to the appropriate concentration to give a final DMSO concentration of 0.5% NMR spectroscopy indicated that the Ru−N bond in the complexes is stable in DMSO−water solution. Then 100 μL of the drug solution was added to each well and the plates were incubated for another 72 h. Subsequently, MTT (5 mg/mL solution) was added to the cells and the plates were incubated for a further 4 h. The culture medium was aspirated, and the purple formazan crystals formed by the mitochondrial dehydrogenase activity of vital cells were dissolved in DMSO. The optical density, directly proportional to the number of surviving cells, was quantified at 540 nm using a multiwell plate reader and the fraction of surviving cells was calculated from the absorbance of untreated control cells. Evaluation is based on means from two independent experiments, each comprising three microcultures per concentration level.

Cell Uptake Measurements. Cells were seeded in 6-well plates, grown to approximately 50% confluency, and incubated with the corresponding compound for the required incubation time. After incubation, cells were detached using an enzyme free dissociation solution (Millipore) and pelleted for 10 min at 100*g* and 4 °C and washed twice with ice-cold PBS. Cell lysis was achieved using a freeze−thaw technique. All samples were analyzed for their protein content prior to ICP-MS determination using a bicinchoninic acid (BCA) assay (Sigma-Aldrich). Quantitation of cells was then possible, with a correlation established for this cell line between the sample total protein content and its number of cells.[54] All determinations described above were carried out as at least two independent experiments. Sample digestion was carried out in concentrated nitric acid for 3 h. Samples were then filled to a total volume of 8 mL with water. Indium was added as an internal standard at a concentration of 0.5 ppb. Determination of internalized metal content was achieved on an Elan DRC II ICP-MS instrument (PerkinElmer, Switzerland) equipped with a Meinhard nebulizer and a cyclonic spray chamber. The ICP-MS instrument was tuned using a solution provided by the manufacturer containing 1 ppb of each element Mg, In, Ce, Ba, Pb, and U. External standards were prepared gravimetrically in an identical matrix to the

dx.doi.org/10.1021/jm5002748 | *J. Med. Chem.* 2014, 57, 3546−3558

samples (with regard to internal standard and nitric acid) with single element standards obtained from CPI International (Amsterdam, The Netherlands).

Apoptosis Assay. A2780 cells were seeded on 6-well plates (2×10^5 cells/well) and grown for 24 h in complete medium before treatment. Compound **1** was freshly dissolved in DMSO, diluted in complete medium, and added to the cells at the final concentrations indicated in Table 4. After incubation for 24 h, apoptosis was measured by flow cytometric determination of subdiploid cells after DNA extraction and subsequent staining with propidium iodide (PI) as described previously.[55] Briefly, cells were harvested and subsequently fixed in 70% ethanol at 20 °C. After 2 h, the cells were resuspended in DNA extraction buffer (45 mM Na_2HPO_4, 2.5 mM citric acid, and 1% Triton X-100, pH 7.4) for 20 min at 37 °C. PI was added to a final concentration of 20 μg/mL, and log scale red fluorescence was analyzed on a FACS Calibur (BD Biosciences, NJ, U.S.).

Wound Assay (Migration). The migration capability of cells was measured using the wound assay.[56] Human breast adenocarcinoma (MDA-MB-231) cells were grown to confluence and cells were labeled with calcein AM (Molecular Probes, C3100MP, Carlsbad, USA) for 15 min (1:2000, Molecular Probes), and "scratch wounds" (with an approximate width of 350 μm) were made in the monolayer by removing cells with a sterile scratch tool (Peira Scientific Instruments, Belgium). Cultures were washed with PBS, and the medium was replaced by fresh medium and incubated with **1** at doses between 6 and 50 μM for 14 h. Plates were scanned using an Acumen eX3 laser scanner cytometer (TTP LabTech Ltd., UK) to record images for computational analysis of scratch sizes using UGR Scratch Assay 6.2 software (DCI Laboratories, Peira Scientific Instruments, Belgium).

Developmental CAM Model. Antiangiogenic efficacy of **1** was tested in the physiologically developing chicken embryo chorioallantoic membrane (CAM) model between embryo development days (EDDs) 11 and 14. Complex **1** was applied by iv injection (50 μM, 100 μL/day for four consecutive days), at EDDs 11, 12, 13, and 14. The control eggs were treated with (100 μL/day of 0.9% NaCl 100 μL/day for four consecutive days). At EDD 15, the CAMs were visualized in ovo using FITC-dextran (20 kDa, 20 μL, 25 mg/mL, Sigma-Aldrich) epifluorescence angiography and subsequently analyzed by the image-processing quantification method described previously.[57] Briefly, on the basis of the FITC-dextran fluorescence angiography, the skeleton of the vascular network is built, and defined descriptors, i.e., branching points (mm^2), give information on the vascular architecture. Five to six eggs were tested per condition. Errors bars represent the standard error of the mean.

Human Ovarian Carcinoma in the CAM. First, 1×10^6 A2780 cells were prepared as a spheroid in a 25 μL hanging drop and 3 h later were transplanted on the surface of the CAM (EDD 7) as described previously.[58] At EDD 11, a solution of **1** in 0.1% DMSO was injected iv at a concentration of 50 μM (100 μL/day) or 2×25 μM (2×50 μL/day, administered with 6 h interval) for four consecutive days. Tumors were measured daily for 8 days. At EDD 17, the experiment was terminated.

Statistical Analysis. Values are given as mean values ± standard deviations (in vitro) or the standard error of the mean (in vivo). Data are represented as averages of independent experiments. Statistical analysis was done using the *t* test (developmental CAM) or two-way Anova (tumor growth curves). *P indicating p-values lower than 0.05 were considered statistically significant.

■ ASSOCIATED CONTENT

Supporting Information

Crystal data and structure refinement for **2**. This material is available free of charge via the Internet at http://pubs.acs.org. Crystallographic information in CIF format of **2** is available on the Internet free of charge under CCDC number 987869 at http://www.ccdc.cam.ac.uk/.

■ AUTHOR INFORMATION

Corresponding Author

*Phone: +41216939854. E-mail: paul.dyson@epfl.ch.

Notes

The authors declare no competing financial interest.

■ ACKNOWLEDGMENTS

We thank the Swiss National Science Foundation, EPFL, and Dr. J. Jacobi for financial support and Euro Solari for the elemental analysis.

■ ABBREVIATIONS USED

CAM, chorioallantoic membrane; DMAP, 4-(dimethylamino)-pyridine; DMSO, dimethyl sulfoxide; EDCI, *N*-(3-(dimethylamino)propyl)-*N*′-ethylcarbodiimide hydrochloride; PI, propidium iodide

■ REFERENCES

(1) Wong, E.; Giandomenico, C. M. Current status of platinum-based antitumor drugs. *Chem. Rev.* **1999**, *99*, 2451−2466.

(2) Jakupec, M. A.; Galanski, M.; Arion, V. B.; Hartinger, C. G.; Keppler, B. K. Antitumour metal compounds: more than theme and variations. *Dalton Trans.* **2008**, 183−194.

(3) Rademaker-Lakhai, J. M.; van den Bongard, D.; Pluim, D.; Beijnen, J. H.; Schellens, J. H. M. A phase I and pharmacological study with imidazolium-*trans*-DMSO-imidazole-tetrachlororuthenate, a novel ruthenium anticancer agent. *Clin. Cancer Res.* **2004**, *10*, 3717−3727.

(4) Hartinger, C. G.; Jakupec, M. A.; Zorbas-Seifried, S.; Groessl, M.; Egger, A.; Berger, W.; Zorbas, H.; Dyson, P. J.; Keppler, B. K. KP1019, a new redox-active anticancer agent—preclinical development and results of a clinical phase I study in tumor patients. *Chem. Biodivers.* **2008**, *5*, 2140−2155.

(5) Bergamo, A.; Sava, G. Ruthenium complexes can target determinants of tumour malignancy. *Dalton Trans.* **2007**, 1267−1272.

(6) Ang, W. H.; Dyson, P. J. Classical and non-classical ruthenium-based anticancer drugs: towards targeted chemotherapy. *Eur. J. Inorg. Chem.* **2006**, *20*, 4003−4018.

(7) Schluga, P.; Hartinger, C. G.; Egger, A.; Reisner, E.; Galanski, M.; Jakupec, M. A.; Keppler, B. K. Redox behavior of tumor-inhibiting ruthenium(III) complexes and effects of physiological reductants on their binding to GMP. *Dalton Trans.* **2006**, 1796−1802.

(8) Clarke, M. J.; Bitler, S.; Rennert, D.; Buchbinder, M.; Kelman, A. D. Reduction and subsequent binding of ruthenium ions catalyzed by subcellular components. *J. Inorg. Biochem.* **1980**, *12*, 79−87.

(9) Wang, D.; Lippard, S. J. Cellular processing of platinum anticancer drugs. *Nature Rev. Drug Discovery* **2005**, *4*, 307−320.

(10) Reedijk, J. New clues for platinum antitumor chemistry: kinetically controlled metal binding to DNA. *Proc. Natl. Acad. Sci. U. S. A.* **2003**, *100*, 3611−3616.

(11) Jamieson, E. R.; Lippard, S. J. Structure, recognition, and processing of cisplatin−DNA adducts. *Chem. Rev.* **1999**, *99*, 2467−2498.

(12) Dyson, P. J. Systematic design of a targeted organometallic antitumour drug in pre-clinical development. *Chimia* **2007**, *61*, 698−703.

(13) Aird, R. E.; Cummings, J.; Ritchie, A. A.; Muir, M.; Morris, R. E.; Chen, H.; Sadler, P. J.; Jodrell, D. I. In vitro and in vivo activity and cross resistance profiles of novel ruthenium (II) organometallic arene complexes in human ovarian cancer. *Br. J. Cancer* **2002**, *86*, 1652−1657.

(14) Habtemariam, A.; Melchart, M.; Fernandez, R.; Parsons, S.; Oswald, I. D. H.; Parkin, A.; Fabbiani, F. P. A.; Davidson, J. E.; Dawson, A.; Aird, R. E.; Jodrell, D. I.; Sadler, P. J. Structure−activity relationships for cytotoxic ruthenium(II) arene complexes containing

N,N-, *N,O*-, and *O,O*-chelating ligands. *J. Med. Chem.* **2006**, *49*, 6858−6868.
(15) Bergamo, A.; Masi, A.; Peacock, A. F. A.; Habtemariam, A.; Sadler, P. J.; Sava, G. In vivo tumour and metastasis reduction and in vitro effects on invasion assays of the ruthenium RM175 and osmium AFAP51 organometallics in the mammary cancer model. *J. Inorg. Biochem.* **2010**, *104*, 79−86.
(16) Scolaro, C.; Bergamo, A.; Brescacin, L.; Delfino, R.; Cocchietto, M.; Laurenczy, G.; Geldbach, T. J.; Sava, G.; Dyson, P. J. In vitro and in vivo evaluation of ruthenium(II)−arene PTA complexes. *J. Med. Chem.* **2005**, *48*, 4161−4171.
(17) Ang, W. H.; Daldini, E.; Scolaro, C.; Scopelliti, R.; Juillerat-Jeannerat, L.; Dyson, P. J. Development of organometallic ruthenium−arene anticancer drugs that resist hydrolysis. *Inorg. Chem.* **2006**, *45*, 9006−9013.
(18) Scolaro, C.; Geldbach, T. J.; Rochat, S.; Dorcier, A.; Gossens, C.; Bergamo, A.; Cocchietto, M.; Tavernelli, I.; Sava, G.; Rothlisberger, U.; Dyson, P. J. Influence of hydrogen-bonding substituents on the cytotoxicity of RAPTA compounds. *Organometallics* **2006**, *25*, 756−765.
(19) Bergamo, A.; Masi, A.; Dyson, P. J.; Sava, G. Modulation of the metastatic progression of breast cancer with an organometallic ruthenium compound. *Int. J. Oncol.* **2008**, *33*, 1281−1289.
(20) Bergamo, A.; Gaiddon, C.; Schellens, J. H. M.; Beijnen, J. H.; Sava, G. Approaching tumour therapy beyond platinum drugs. Status of the art and perspectives of ruthenium drug candidates. *J. Inorg. Biochem.* **2012**, *106*, 90−99.
(21) Nowak-Sliwinska, P.; van Beijnum, J. R.; Casini, A.; Nazarov, A. A.; Wagnieres, G.; van den Bergh, H.; Dyson, P. J.; Griffioen, A. W. Organometallic ruthenium(II) arene compounds with antiangiogenic activity. *J. Med. Chem.* **2011**, *54*, 3895−3902.
(22) Vock, C. A.; Scolaro, C.; Phillips, A. D.; Scopelliti, R.; Sava, G.; Dyson, P. J. Synthesis, characterization, and in vitro evaluation of novel ruthenium(II) η^6-arene imidazole complexes. *J. Med. Chem.* **2006**, *49*, 5552−5561.
(23) Casini, A.; Gabbiani, C.; Sorrentino, F.; Rigobello, M. P.; Bindoli, A.; Geldbach, T. J.; Marrone, A.; Re, N.; Hartinger, C. G.; Dyson, P. J.; Messori, L. Emerging protein targets for anticancer metallodrugs: inhibition of thioredoxin reductase and cathepsin B by antitumor ruthenium(II)−arene compounds. *J. Med. Chem.* **2008**, *51*, 6773−6781.
(24) Casini, A.; Karotki, A.; Gabbiani, C.; Rugi, F.; Vasak, M.; Messori, L.; Dyson, P. J. Reactivity of an antimetastatic organometallic ruthenium compound with metallothionein-2: relevance to the mechanism of action. *Metallomics* **2009**, *1*, 434−441.
(25) Wu, B.; Ong, M. S.; Groessl, M.; Adhireksan, Z.; Hartinger, C. G.; Dyson, P. J.; Davey, C. A. A ruthenium antimetastasis agent forms specific histone protein adducts in the nucleosome core. *Chem.—Eur. J.* **2011**, *17*, 3562−3566.
(26) Nazarov, A. A.; Risse, J.; Ang, W. H.; Schmitt, F.; Zava, O.; Ruggi, A.; Groessl, M.; Scopelitti, R.; Juillerat-Jeanneret, L.; Hartinger, C. G.; Dyson, P. J. Anthracene-tethered ruthenium(II) arene complexes as tools to visualize the cellular localization of putative organometallic anticancer compounds. *Inorg. Chem.* **2012**, *51*, 3633−3639.
(27) Tan, Y. Q.; Dyson, P. J.; Ang, W. H. Acetal-functionalized RAPTA complexes for conjugation and labeling. *Organometallics* **2011**, *30*, 5965−5971.
(28) Ang, W. H.; De Luca, A.; Chapuis-Bernasconi, C.; Juillerat-Jeanneret, L.; Lo Bello, M.; Dyson, P. J. Organometallic ruthenium inhibitors of glutathione-*S*-transferase P1−1 as anticancer drugs. *ChemMedChem* **2007**, *2*, 1799−1806.
(29) Ang, W. H.; Parker, L. J.; De Luca, A.; Juillerat-Jeanneret, L.; Morton, C. J.; Lo Bello, M.; Parker, M. W.; Dyson, P. J. Rational design of an organometallic glutathione transferase inhibitor. *Angew. Chem. Int. Ed.* **2009**, *48*, 3854−3857.
(30) Hanif, M.; Meier, S. M.; Kandioller, W.; Bytzek, A.; Hejl, M.; Hartinger, C. G.; Nazarov, A. A.; Arion, V. B.; Jakupec, M. A.; Dyson, P. J.; Keppler, B. K. From hydrolytically labile to hydrolytically stable Ru(II)−arene anticancer complexes with carbohydrate-derived co-ligands. *J. Inorg. Biochem.* **2011**, *105*, 224−231.
(31) Kilpin, K. J.; Clavel, C. M.; Edafe, F.; Dyson, P. J. Naphthalimide-tagged ruthenium−arene anticancer complexes: combining coordination with intercalation. *Organometallics* **2012**, *31*, 7031−7039.
(32) Ang, W. H.; Daldini, E.; Juillerat-Jeanneret, L.; Dyson, P. J. Strategy to tether organometallic ruthenium−arene anticancer compounds to recombinant human serum albumin. *Inorg. Chem.* **2007**, *46*, 9048−9050.
(33) Clavel, C. M.; Paunescu, E.; Nowak-Sliwinska, P.; Dyson, P. J. Thermoresponsive organometallic arene ruthenium complexes for tumour targeting. *Chem. Sci.* **2014**, *5*, 1097−1101.
(34) Jost, L. M.; Gschwind, H. P.; Jalava, T.; Wang, Y. Y.; Guenther, C.; Souppart, C.; Rottmann, A.; Denner, K.; Waldmeier, F.; Gross, G.; Masson, E.; Laurent, D. Metabolism and disposition of vatalanib (PTK787/ZK-222584) in cancer patients. *Drug. Metab. Dispos.* **2006**, *34*, 1817−1828.
(35) Wang, F. Y.; Habtemariam, A.; van der Geer, E. P. L.; Fernandez, R.; Melchart, M.; Deeth, R. J.; Aird, R.; Guichard, S.; Fabbiani, F. P. A.; Lozano-Casal, P.; Oswald, I. D. H.; Jodrell, D. I.; Parsons, S.; Sadler, P. J. Controlling ligand substitution reactions of organometallic complexes: tuning cancer cell cytotoxicity. *Proc. Natl. Acad. Sci. U. S. A.* **2005**, *102*, 18269−18274.
(36) Renfrew, A. K.; Phillips, A. D.; Egger, A. E.; Hartinger, C. G.; Bosquain, S. S.; Nazarov, A. A.; Keppler, B. K.; Gonsalvi, L.; Peruzzini, M.; Dyson, P. J. Influence of structural variation on the anticancer activity of RAPTA-type complexes: ptn versus pta. *Organometallics* **2009**, *28*, 1165−1172.
(37) Dorcier, A.; Dyson, P. J.; Gossens, C.; Rothlisberger, U.; Scopelliti, R.; Tavernelli, I. Binding of organometallic ruthenium(II) and osmium(II) complexes to an oligonucleotide: a combined mass spectrometric and theoretical study. *Organometallics* **2005**, *24*, 2114−2123.
(38) Allardyce, C. S.; Dyson, P. J.; Ellis, D. J.; Heath, S. L. [Ru(η^6-*p*-cymene)Cl_2(pta)] (pta=1,3,5-triaza-7-phosphatricyclo[3.3.1.1]-decane): a water soluble compound that exhibits pH dependent DNA binding providing selectivity for diseased cells. *Chem. Commun.* **2001**, 1396−1397.
(39) Ang, W. H. Novel Strategies for ovecoming Drug Resistance in Transitional Metal-Based Anticancer Compounds. Ph.D. Thesis . École Polytechnique Fédérale de Lausanne, 2007.
(40) Kilpin, K. J.; Crot, S.; Riedel, T.; Kitchen, J. A.; Dyson, P. J. Ruthenium(II) and osmium(II) 1,2,3-triazolylidene organometallics: a preliminary investigation into the biological activity of 'click' carbene complexes. *Dalton Trans.* **2014**, *43*, 1443−1448.
(41) Nazarov, A. A.; Baquie, M.; Nowak-Sliwinska, P.; Zava, O.; van Beijnum, J. R.; Groessl, M.; Chisholm, D. M.; Ahmadi, Z.; McIndoe, J. S.; Griffioen, A. W.; van den Bergh, H.; Dyson, P. J. Synthesis and characterization of a new class of anti-angiogenic agents based on ruthenium clusters. *Sci. Rep.* **2013**, *3*, 1485.
(42) Capozzi, I.; Clerici, K.; Cocchietto, M.; Salerno, G.; Bergamo, A.; Sava, G. Modification of cell cycle and viability of TLX5 lymphoma in vitro by sulfoxide−ruthenium compounds and cisplatin detected by flow cytometry. *Chem.−Biol. Interact.* **1998**, *113*, 51−64.
(43) Nowak-Sliwinska, P.; Weiss, A.; Beijnum, J. R.; Wong, T. J.; Ballini, J. P.; Lovisa, B.; van den Bergh, H.; Griffioen, A. W. Angiostatic kinase inhibitors to sustain photodynamic angio-occlusion. *J. Cell. Mol. Med.* **2012**, *16*, 1553−1562.
(44) Scolaro, C.; Bergamo, A.; Brescacin, L.; Delfino, R.; Cocchietto, M.; Laurenczy, G.; Geldbach, T. J.; Sava, G.; Dyson, P. J. In vitro and in vivo evaluation of ruthenium(II)−arene PTA complexes. *J. Med. Chem.* **2005**, *48*, 4161−4171.
(45) Hartinger, C. G.; Metzler-Nolte, N.; Dyson, P. J. Challenges and opportunities in the development of organometallic anticancer drugs. *Organometallics* **2012**, *31*, 5677−5685.
(46) Bennett, M. A.; Smith, A. K. Arene ruthenium(II) complexes formed by dehydrogenation of cyclohexadienes with ruthenium(III) trichloride. *J. Chem. Soc., Dalton Trans.* **1974**, 233−241.

(47) Vriamont, N.; Govaerts, B.; Grenouillet, P.; de Bellefon, C.; Riant, O. Design of a Genetic Algorithm for the Simulated Evolution of a Library of Asymmetric Transfer Hydrogenation Catalysts. *Chem.—Eur. J.* **2009**, *15*, 6267−6278.
(48) Lalrempuia, R.; Kollipara, M. R. Reactivity studies of η^6-arene ruthenium (II) dimers with polypyridyl ligands: isolation of mono, binuclear *p*-cymene ruthenium (II) complexes and bisterpyridine ruthenium (II) complexes. *Polyhedron* **2003**, *22*, 3155−3160.
(49) Bennett, M. A.; Matheson, T. W.; Robertson, G. B.; Smith, A. K.; Tucker, P. A. Highly fluxional arene cyclooctatetraene complexes of zerovalent iron, ruthenium, and osmium—single-crystal X-ray study of (cyclooctatetraene)(hexamethylbezene)ruthenium(0), Ru(Eta-6-Hmb)(1−4-Eta-Cot). *Inorg. Chem.* **1980**, *19*, 1014−1021.
(50) Nongbri, S. L.; Das, B.; Rao, K. M. Arene ruthenium beta-diketonato triazolato derivatives: synthesis and spectral studies (beta-diketones: 1-phenyl-3-methyl-4-benzoyl pyrazol-5-one, acetylacetone derivatives). *J. Organomet. Chem.* **2009**, *694*, 3881−3891.
(51) Fulmer, G. R.; Miller, A. J. M.; Sherden, N. H.; Gottlieb, H. E.; Nudelman, A.; Stoltz, B. M.; Bercaw, J. E.; Goldberg, K. I. NMR chemical shifts of trace impurities: common laboratory solvents, organics, and gases in deuterated solvents relevant to the organometallic chemist. *Organometallics* **2010**, *29*, 2176−2179.
(52) *Automar*, release 2.8.0; Marresearch GmbH: Norderstedt, Germany, 2011.
(53) Sheldrick, G. M. A short history of SHELX. *Acta Crystallogr., Sect. A: Found. Crystallogr.* **2008**, *64*, 112−122.
(54) Tuszynski, G. P.; Murphy, A. Spectrophotometric quantitation of anchorage-dependent cell numbers using the bicinchoninic acid protein assay reagent. *Anal. Biochem.* **1990**, *184*, 189−191.
(55) van Beijnum, J. R.; Nowak-Sliwinska, P.; van den Boezem, E.; Hautvast, P.; Buurman, W. A.; Griffioen, A. W. Tumor angiogenesis is enforced by autocrine regulation of high-mobility group box 1. *Oncogene* **2013**, *17*, 363−374.
(56) Weiss, A.; van Beijnum, J. R.; Bonvin, D.; Jichlinski, P.; Dyson, P. J.; Griffioen, A. W.; Nowak-Sliwinska, P. Low-dose angiostatic tyrosine kinase inhibitors improve photodynamic therapy for cancer: lack of vascular normalization. *J. Cell. Mol. Med.* **2014**, *18*, 480−491.
(57) Nowak-Sliwinska, P.; Ballini, J. P.; Wagnieres, G.; van den Bergh, H. Processing of fluorescence angiograms for the quantification of vascular effects induced by anti-angiogenic agents in the CAM model. *Microvasc. Res.* **2010**, *79*, 21−28.
(58) Adar, Y.; Stark, M.; Bram, E. E.; Nowak-Sliwinska, P.; van den Bergh, H.; Szewczyk, G.; Sarna, T.; Skladanowski, A.; Griffioen, A. W.; Assaraf, Y. G. Imidazoacridinone-dependent lysosomal photodestruction: a pharmacological Trojan horse approach to eradicate multidrug-resistant cancers. *Cell Death Differ.* **2012**, *3*, e293.